Efficient Generation of Functional Hepatocytes From Human Embryonic Stem Cells and Induced Pluripotent Stem Cells by HNF4α Transduction

Kazuo Takayama[1,2], Mitsuru Inamura[1,2], Kenji Kawabata[2,3], Kazufumi Katayama[1], Maiko Higuchi[2], Katsuhisa Tashiro[2], Aki Nonaka[2], Fuminori Sakurai[1], Takao Hayakawa[4,5], Miho Kusuda Furue[6,7] and Hiroyuki Mizuguchi[1,2,8]

[1]Laboratory of Biochemistry and Molecular Biology, Graduate School of Pharmaceutical Sciences, Osaka University, Osaka, Japan; [2]Laboratory of Stem Cell Regulation, National Institute of Biomedical Innovation, Osaka, Japan; [3]Laboratory of Biomedical Innovation, Graduate School of Pharmaceutical Sciences, Osaka University, Osaka, Japan; [4]Pharmaceutics and Medical Devices Agency, Tokyo, Japan; [5]Pharmaceutical Research and Technology Institute, Kinki University, Osaka, Japan; [6]JCRB Cell Bank, Division of Bioresources, National Institute of Biomedical Innovation, Osaka, Japan; [7]Laboratory of Cell Processing, Institute for Frontier Medical Sciences, Kyoto University, Kyoto, Japan; [8]The Center for Advanced Medical Engineering and Informatics, Osaka University, Osaka, Japan

Hepatocyte-like cells from human embryonic stem cells (ESCs) and induced pluripotent stem cells (iPSCs) are expected to be a useful source of cells drug discovery. Although we recently reported that hepatic commitment is promoted by transduction of SOX17 and HEX into human ESC- and iPSC-derived cells, these hepatocyte-like cells were not sufficiently mature for drug screening. To promote hepatic maturation, we utilized transduction of the hepatocyte nuclear factor 4α (HNF4α) gene, which is known as a master regulator of liver-specific gene expression. Adenovirus vector-mediated overexpression of HNF4α in hepatoblasts induced by SOX17 and HEX transduction led to upregulation of epithelial and mature hepatic markers such as cytochrome P450 (CYP) enzymes, and promoted hepatic maturation by activating the mesenchymal-to-epithelial transition (MET). Thus HNF4α might play an important role in the hepatic differentiation from human ESC-derived hepatoblasts by activating the MET. Furthermore, the hepatocyte like-cells could catalyze the toxication of several compounds. Our method would be a valuable tool for the efficient generation of functional hepatocytes derived from human ESCs and iPSCs, and the hepatocyte-like cells could be used for predicting drug toxicity.

Received 19 July 2011; accepted 28 September 2011; published online 8 November 2011. doi:10.1038/mt.2011.234

INTRODUCTION

Human embryonic stem cells (ESCs) and induced pluripotent stem cells (iPSCs) are able to replicate indefinitely and differentiate into most of the body's cell types.[1,2] They could provide an unlimited source of cells for various applications. Hepatocyte-like cells, which are differentiated from human ESCs and iPSCs, would be useful for basic research, regenerative medicine, and drug discovery.[3] In particular, it is expected that hepatocyte-like cells will be utilized as a tool for cytotoxicity screening in the early phase of pharmaceutical development. To catalyze the toxication of several compounds, hepatocyte-like cells need to be mature enough to exhibit hepatic functions, including high activity levels of the cytochrome P450 (CYP) enzymes. Because the present technology for the generation of hepatocyte-like cells from human ESCs and iPSCs, which is expected to be utilized for drug discovery, is not refined enough for this application, it is necessary to improve the efficiency of hepatic differentiation. Although conventional methods such as growth factor-mediated hepatic differentiation are useful to recapitulate liver development, they lead to only a heterogeneous hepatocyte population.[4–6] Recently, we showed that transcription factors are transiently transduced to promote hepatic differentiation in addition to the conventional differentiation method which uses only growth factors.[7] Ectopic expression of Sry-related HMG box 17 (SOX17) or hematopoietically expressed homeobox (HEX) by adenovirus (Ad) vectors in human ESC-derived mesendoderm or definitive endoderm (DE) cells markedly enhances the endoderm differentiation or hepatic commitment, respectively.[7,8] However, further hepatic maturation is required for drug screening.

The transcription factor hepatocyte nuclear factor 4α (HNF4α) is initially expressed in the developing hepatic diverticulum on E8.75,[9,10] and its expression is elevated as the liver develops. A previous loss-of-function study showed that HNF4α plays a critical role in liver development; conditional deletion of *HNF4α* in fetal hepatocytes results in the faint expression of many mature hepatic enzymes and the impairment of normal liver morphology.[11] The genome-scale chromatin immunoprecipitation assay showed that HNF4α binds to the promoters of nearly half of the genes expressed in the mouse liver,[12] including cell adhesion and junctional proteins,[13] which are important in

Correspondence: Hiroyuki Mizuguchi, Laboratory of Biochemistry and Molecular Biology, Graduate School of Pharmaceutical Sciences, Osaka University, 1-6 Yamadaoka, Suita, Osaka 565-0871, Japan. E-mail: mizuguch@phs.osaka-u.ac.jp

the hepatocyte epithelial structure.[14] In addition, HNF4α plays a critical role in hepatic differentiation and in a wide variety of liver functions, including lipid and glucose metabolism.[15,16] Although HNF4α could promote transdifferentiation into hepatic lineage from hematopoietic cells,[17] the function of HNF4α in hepatic differentiation from human ESCs and iPSCs remains unknown. A previous study showed that hepatic differentiation from mouse hepatic progenitor cells is promoted by HNF4α, although many of the hepatic markers that they examined were target genes of HNF4α.[18] They transplanted the HNF4α-overexpressed mouse hepatic progenitor cells to promote hepatic differentiation, but they did not examine the markers that relate to hepatic maturation such as CYP enzymes, conjugating enzymes, and hepatic transporters.

In this study, we examined the role of HNF4α in hepatic differentiation from human ESCs and iPSCs. The human ESC- and iPSC-derived hepatoblasts, which were efficiently generated by sequential transduction of SOX17 and HEX, were transduced with HNF4α-expressing Ad vector (Ad-HNF4α), and then the expression of hepatic markers of the hepatocyte-like cells were assessed. In addition, we examined whether or not the hepatocyte-like cells, which were generated by sequential transduction of SOX17, HEX, and HNF4α, were able to predict the toxicity of several compounds.

RESULTS

Stage-specific HNF4α transduction in hepatoblasts selectively promotes hepatic differentiation

The transcription factor HNF4α plays an important role in both liver generation[11] and hepatic differentiation from human ESCs and iPSCs (**Supplementary Figure S1**). We expected that hepatic differentiation could be accelerated by HNF4α transduction. To examine the effect of forced expression of HNF4α in the hepatic differentiation from human ESC- and iPSC-derived cells, we used a fiber-modified Ad vector.[19] Initially, we optimized the time period for Ad-HNF4α transduction. Human ESC (H9)-derived DE cells (day 6) (**Supplementary Figures S2** and **S3a**), hepatoblasts (day 9) (**Supplementary Figures S2** and **S3b**), or a heterogeneous population consisting of hepatoblasts, hepatocytes, and cholangiocytes (day 12) (**Supplementary Figures S2** and **S3c**) were transduced with Ad-HNF4α and then the Ad-HNF4α-transduced cells were cultured until day 20 of differentiation (**Figure 1**). We ascertained the expression of exogenous *HNF4α* in human ESC-derived hepatoblasts (day 9) transduced with Ad-HNF4α (**Supplementary Figure S4**). The transduction of Ad-HNF4α into human ESC-derived hepatoblasts (day 9) led to the highest expression levels of the hepatocyte markers *albumin* (*ALB*)[20] and *α-1-antitrypsin* (**Figure 1a**). In contrast, the expression levels of the cholangiocyte markers *cytokeratin 7* (*CK7*)[21] and *SOX9*[22] were

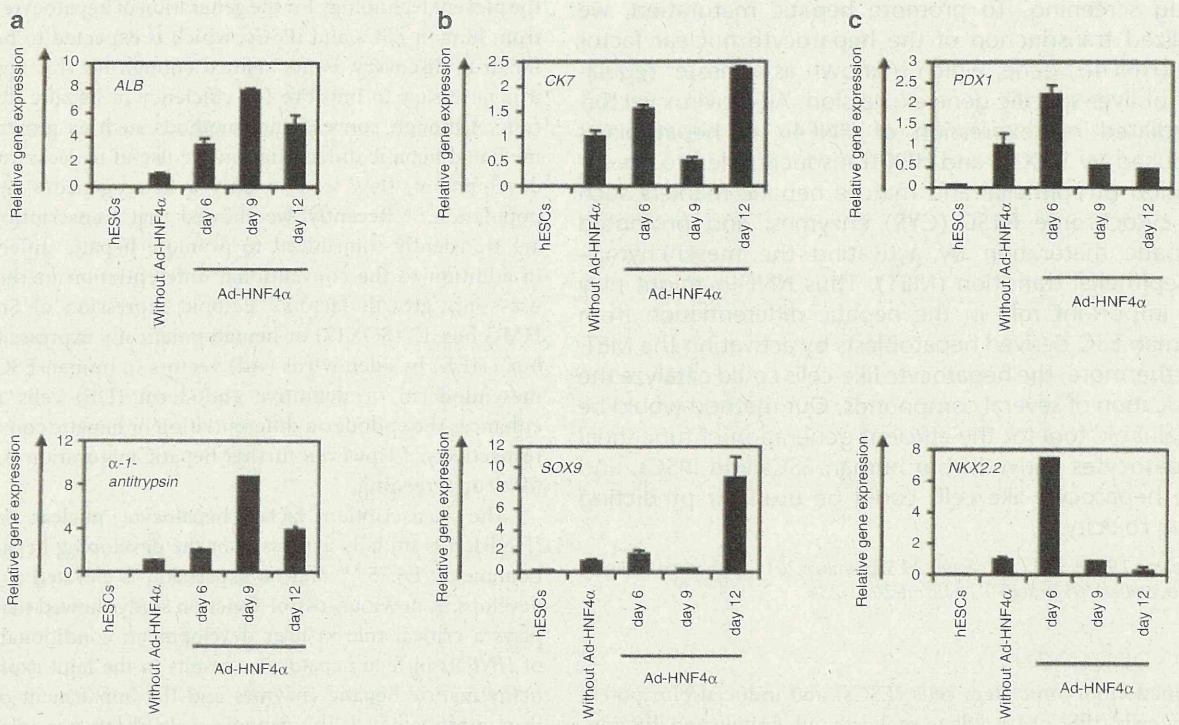

Figure 1 Transduction of HNF4α into hepatoblasts promotes hepatic differentiation. (**a**–**c**) The human ESC (H9)-derived cells, which were cultured for 6, 9, or 12 days according to the protocol described in **Figure 2a**, were transduced with 3,000 vector particles (VP)/cell of Ad-HNF4α for 1.5 hours and cultured until day 20. The gene expression levels of (**a**) hepatocyte markers (*ALB* and *α-1-antitrypsin*), (**b**) cholangiocyte markers (*CK7* and *SOX9*), and (**c**) pancreas markers (*PDX1* and *NKX2.2*) were examined by real-time RT-PCR on day 0 (human ESCs (hESCs)) or day 20 of differentiation. The horizontal axis represents the days when the cells were transduced with Ad-HNF4α. On the y-axis, the level of the cells without Ad-HNF4α transduction on day 20 was taken as 1.0. All data are represented as means ± SD (n = 3). ESC, embryonic stem cell; HNF4α, hepatocyte nuclear factor 4α; RT-PCR, reverse transcription-PCR.

downregulated in the cells transduced on day 9 as compared with nontransduced cells (**Figure 1b**). This might be because hepatic differentiation was selectively promoted and biliary differentiation was repressed by the transduction of HNF4α in hepatoblasts. The expression levels of the pancreas markers *PDX1*[23] and *NKX2.2*[24] did not make any change in the cells transduced on day 9 as compared with nontransduced cells (**Figure 1c**). Interestingly, the expression levels of the pancreas markers were upregulated, when Ad-HNF4α transduction was performed into DE cells (day 6) (**Figure 1c**). These results suggest that HNF4α might promote not only hepatic differentiation but also pancreatic differentiation, although the optimal stage of HNF4 transduction for the differentiation of each cell is different. We have confirmed that there was no difference between nontransduced cells and Ad-LacZ-transduced cells in the gene expression levels of all the markers investigated in **Figure 1a–c** (data not shown). We also confirmed that Ad vector-mediated gene expression in the human ESC-derived hepatoblasts (day 9) continued until day 14 and almost disappeared on day 18 (**Supplementary Figure S5**). These results indicated that the stage-specific HNF4α overexpression in human ESC-derived hepatoblasts (day 9) was essential for promoting efficient hepatic differentiation.

Transduction of HNF4α into human ESC- and iPSC-derived hepatoblasts efficiently promotes hepatic maturation

From the results of **Figure 1**, we decided to transduce hepatoblasts (day 9) with Ad-HNF4α. To determine whether hepatic maturation is promoted by Ad-HNF4α transduction, Ad-HNF4α-transduced cells were cultured until day 20 of differentiation according to the schematic protocol described in **Figure 2a**. After the hepatic maturation, the morphology of human ESCs was gradually changed into that of hepatocytes: polygonal with distinct round nuclei (day 20) (**Figure 2b**). Interestingly, a portion of the hepatocyte-like cells, which were ALB[20]-, CK18[21]-, CYP2D6-, and CYP3A4[25]-positive cells, had double nuclei, which was also observed in primary human hepatocytes (**Figure 2b,c**, and **Supplementary Figure S6**). We also examined the hepatic gene expression levels on day 20 of differentiation (**Figure 3a,b**). The gene expression analysis of *CYP1A2*, *CYP2C9*, *CYP2C19*, *CYP2D6*, *CYP3A4*, and *CYP7A1*[25] showed higher expression levels in all of Ad-SOX17-, Ad-HEX-, and Ad-HNF4α-transduced cells (three factors-transduced cells) as compared with those in both Ad-SOX17- and Ad-HEX-transduced cells (two factors-transduced cells) on day 20 (**Figure 3a**). The gene expression level of NADPH-CYP reductase

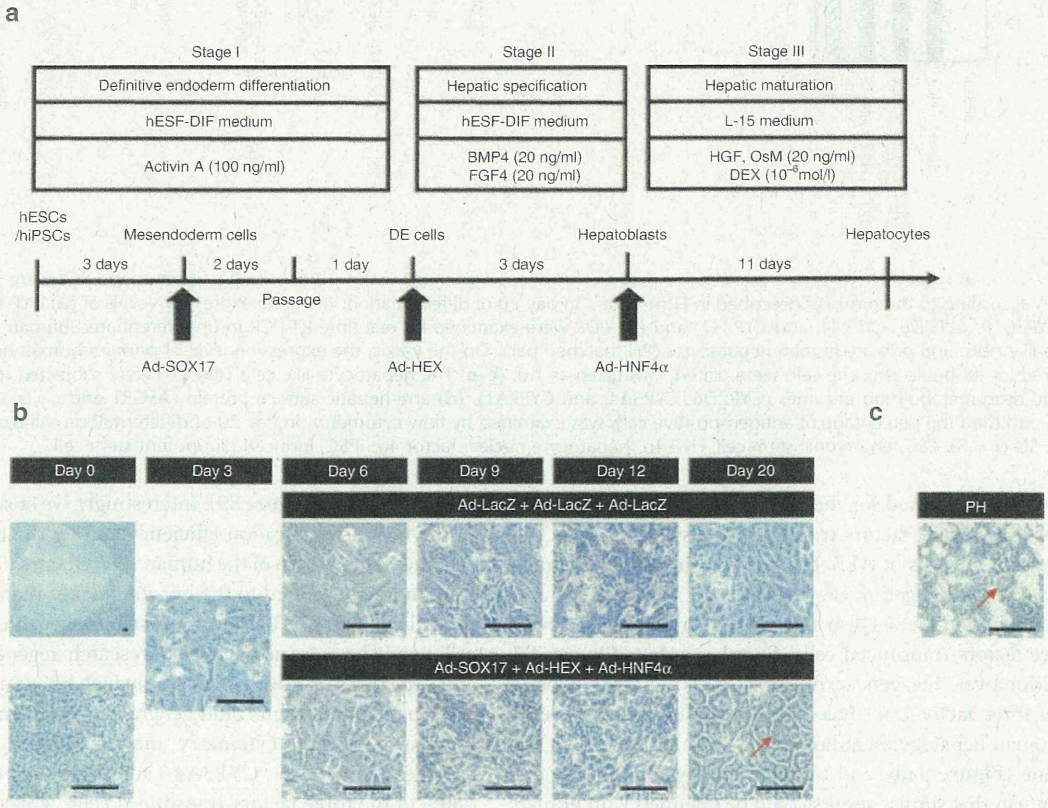

Figure 2 Hepatic differentiation of human ESCs and iPSCs transduced with three factors. (**a**) The procedure for differentiation of human ESCs and iPSCs into hepatocytes via DE cells and hepatoblasts is presented schematically. The hESF-DIF medium was supplemented with 10 μg/ml human recombinant insulin, 5 μg/ml human apotransferrin, 10 μmol/l 2-mercaptoethanol, 10 μmol/l ethanolamine, 10 μmol/l sodium selenite, and 0.5 mg/ml fatty-acid-free BSA. The L15 medium was supplemented with 8.3% tryptose phosphate broth, 8.3% FBS, 10 μmol/l hydrocortisone 21-hemisuccinate, 1 μmol/l insulin, and 25 mmol/l $NaHCO_3$. (**b**) Sequential morphological changes (day 0–20) of human ESCs (H9) differentiated into hepatocytes via DE cells and hepatoblasts are shown. Red arrow shows the cells that have double nuclei. (**c**) The morphology of primary human hepatocytes is shown. Bar represents 50 μm. BSA, bovine serum albumin; DE, definitive endoderm; ESC, embryonic stem cell; iPSC, induced pluripotent stem cell.

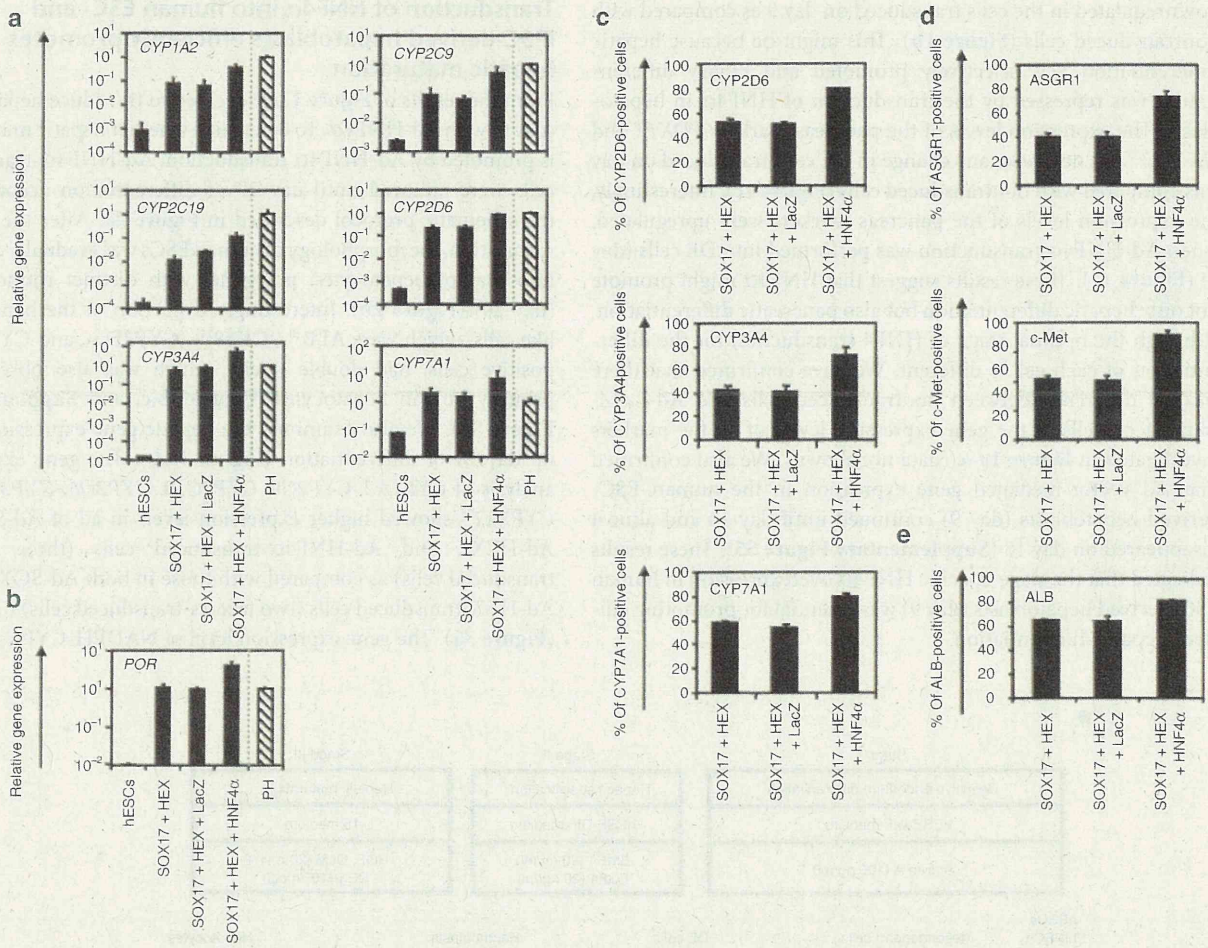

Figure 3 Transduction of HNF4α promotes hepatic maturation from human ESCs and iPSCs. (**a**,**b**) The human ESCs were differentiated into hepatocytes according to the protocol described in **Figure 2a**. On day 20 of differentiation, the gene expression levels of (**a**) CYP enzymes (*CYP1A2*, *CYP2C9*, *CYP2C19*, *CYP2D6*, *CYP3A4*, and *CYP7A1*) and (**b**) *POR* were examined by real-time RT-PCR in undifferentiated human ESCs (hESCs), the hepatocyte-like cells, and primary human hepatocytes (PH, hatched bar). On the y-axis, the expression level of primary human hepatocytes, which were cultured for 48 hours after the cells were plated, was taken as 1.0. (**c**–**e**) The hepatocyte-like cells (day 20) were subjected to immunostaining with (**c**) anti-drug-metabolizing enzymes (CYP2D6, CYP3A4, and CYP7A1), (**d**) anti-hepatic surface protein (ASGR1 and c-Met), and (**e**) anti-ALB antibodies, and then the percentage of antigen-positive cells was examined by flow cytometry on day 20 of differentiation. All data are represented as means ± SD ($n = 3$). ESC, embryonic stem cell; HNF4α, hepatocyte nuclear factor 4α; iPSC, induced pluripotent stem cell.

(POR)[26], which is required for the normal function of CYPs, was also higher in the three factors-transduced cells (**Figure 3b**). The gene expression analysis of ALB, α-1-antitrypsin (α-1-AT), transthyretin, hepatic conjugating enzymes, hepatic transporters, and hepatic transcription factors also showed higher expression levels in the three factors-transduced cells (**Supplementary Figures S7** and **S8**). Moreover, the gene expression levels of these hepatic markers of three factor-transduced cells were similar to those of primary human hepatocytes, although the levels depended on the type of gene (**Figure 3a,b**, and **Supplementary Figures S7** and **S8**). To confirm that similar results could be obtained with human iPSCs, we used three human iPS cell lines (201B7, Dotcom, and Tic). The gene expression of hepatic markers in human ESC- and iPSC-derived hepatocytes were analyzed by real-time reverse transcription-PCR on day 20 of differentiation. Three human iPS cell lines as well as human ESCs also effectively differentiated into hepatocytes in response to transduction of the three factors (**Supplementary Figure S9**). Interestingly, we observed differences in the hepatic maturation efficiency among the three human iPS cell lines. That is, two of the human iPS cell lines (Tic and Dotcom) were more committed to the hepatic lineage than another human iPS cell line (201B7). Because almost homogeneous hepatocyte-like cells would be more useful in basic research, regenerative medicine, and drug discovery, we also examined whether our novel methods for hepatic maturation could generate a homogeneous hepatocyte population by flow cytometry analysis (**Figure 3c–e**). The percentages of CYP2D6-, CYP3A4-, and CYP7A1-positive cells were ~80% in the three factors-transduced cells, while they were ~50% in the two factors-transduced cells (**Figure 3c**). The percentages of hepatic surface antigen (asialoglycoprotein receptor 1 (ASGR1] and met proto-oncogene (c-Met))-positive cells (**Figure 3d**) and ALB-positive cells (**Figure 3e**) were also ~80% in the three factors-transduced cells. These results indicated that a nearly homogeneous population was obtained by our differentiation protocol

using the transduction of three functional genes (SOX17, HEX, and HNF4α).

The three factors-transduced cells have characteristics of functional hepatocytes

The hepatic functions of the hepatocyte-like cells, such as the uptake of low-density lipoprotein (LDL) and CYP enzymes activity, of the hepatocyte-like cells were examined on day 20 of differentiation. Approximately 87% of the three factors-transduced cells uptook LDL in the medium, whereas only 44% of the two factors-transduced cells did so (**Figure 4a**). The activities of CYP enzymes of the hepatocyte-like cells were measured according to the metabolism of the CYP3A4, CYP2C9, or CYP1A2 substrates (**Figure 4b**). The metabolites were detected in the three factors-transduced cells and their activities were higher than those of the two factors-transduced cells (dimethyl sulfoxide (DMSO) column). We further tested the induction of CYP3A4, CYP2C9, and CYP1A2 by chemical stimulation, since CYP3A4, CYP2C9, and CYP1A2 are the important prevalent CYP isozymes in the liver and are involved in the metabolism of a significant proportion of the currently available commercial drugs (rifampicin or omeprazole column). It is well known that CYP3A4 and CYP2C9 can be induced by rifampicin, whereas CYP1A2 can be induced by omeprazole. The hepatocyte-like cells were treated with either of these. Although undifferentiated human ESCs responsed to neither rifampicin nor omeprazole (data not shown), the hepatocyte-like cells produced more metabolites in response to chemical stimulation as well as primary hepatocytes (**Figure 4b**). The activity levels of the hepatocyte-like cells as compared with those of primary human hepatocytes depended on the types of CYP; the CYP3A4 activity of the hepatocyte-like cells was similar to that of primary human hepatocytes, whereas the CYP2C9 and CYP1A2 activities of the hepatocyte-like cells were slightly lower than those of primary human hepatocytes (**Figure 3a**). These results indicated that high levels of functional CYP enzymes were detectable in the hepatocyte-like cells.

The metabolism of diverse compounds involving uptake, conjugation, and the subsequent release of the compounds is an important function of hepatocytes. Uptake and release of Indocyanine green (ICG) can often be used to identify hepatocytes in ESC differentiation models.[27] To investigate this function in our hepatocyte-like cells, we compared this ability of the three factors-transduced cells with that of the two factors-transduced cells on day 20 of differentiation (**Figure 4c**). The three factors-transduced cells had more ability to uptake ICG and to excrete ICG by culturing without ICG for 6 hours. We also examined whether the hepatocyte-like cells could store glycogen, a characteristic of functional hepatocytes (**Figure 4d**). On day 20 of differentiation, the three factors-transduced cells and the two factors-transduced cells were stained for cytoplasmic glycogen using the Periodic Acid-Schiff staining procedure. The three factors-transduced cells exhibited more abundant storage of glycogen than the two-factors-transduced cells. These results showed that abundant hepatic functions, such as uptake and excretion of ICG and storage of glycogen, were obtained by the transduction of three factors.

Many adverse drug reactions are caused by the CYP-dependent activation of drugs into reactive metabolites.[28] In order to examine metabolism-mediated toxicity and to improve the safety of drug candidates, primary human hepatocytes are widely used.[28] Because primary human hepatocytes have quite different characteristics among distinct lots and because it is difficult to purchase large amounts of primary human hepatocytes that have the same characteristics, hepatocyte-like cells are expected to be used for this purpose. To examine whether our hepatocyte-like cells could be used to predict metabolism-mediated toxicity, the hepatocyte-like cells were incubated with four substrates (troglitazone, acetaminophen, cyclophosphamide, and carbamazepine), which are known to generate toxic metabolites by CYP enzymes, and then the cell viability was measured (**Figure 4e**). The cell viability of the two factors plus Ad-LacZ-tansduced cells were higher than that of the three factors-transduced cells at each different concentration of four test compounds. These results indicated that the three factors-transduced cells could more efficiently metabolize the test compounds and thereby induce higher toxicity than either the two factors-transduced cells or undifferentiated human ESCs. The cell viability of the three factors-transduced cells was slightly higher than that of primary human hepatocytes.

HNF4α promotes hepatic maturation by activating mesenchymal-to-epithelial transition

HNF4α is known as a dominant regulator of the epithelial phenotype because its ectopic expression in fibroblasts (such as NIH 3T3 cells) induces mesenchymal-to-epithelial transition (MET)[11], although it is not known whether HNF4α can promote MET in hepatic differentiation. Therefore, we examined whether HNF4α transduction promotes hepatic maturation from hepatoblasts by activating MET. To clarify whether MET is activated by HNF4α transduction, the human ESC-derived hepatoblasts (day 9) were transduced with Ad-LacZ or Ad-HNF4α, and the resulting phenotype was analyzed on day 12 of differentiation (**Figure 5**). This time, we confirmed that HNF4α transduction decreased the population of N-cadherin (hepatoblast marker)-positive cells,[29] whereas it increased that of ALB (hepatocyte marker)-positive cells (**Figure 5a**). The number of CK7 (cholangiocyte marker)-positive population did not change (**Figure 5a**). To investigate whether these results were attributable to MET, the alteration of the expression of several mesenchymal and epithelial markers was examined (**Figure 5b**). The human ESC-derived hepatoblasts (day 9) were almost homogeneously N-cadherin[30] (mesenchymal marker)-positive and E-cadherin[11] (epithelial marker)-negative, demonstrating that human ESC-derived hepatoblasts have mesenchymal characteristics (**Figure 5a,b**). After HNF4α transduction, the number of E-cadherin-positive cells was increased and reached ~90% on day 20, whereas that of N-cadherin-positive cells was decreased and was less than 5% on day 20 (**Supplementary Figure S10**). These results indicated that MET was promoted by HNF4α transduction in hepatic differentiation from hepatoblasts. Interestingly, the number of growing cells was decreased by HNF4α transduction (**Figure 5c**), and the cell growth was delayed by HNF4α transduction (**Supplementary Figure S11**). This decrease in the number of growing cells might have been because the differentiation was promoted by HNF4α transduction. We also confirmed that MET was promoted by HNF4α transduction in the gene expression levels (**Figure 5d**).

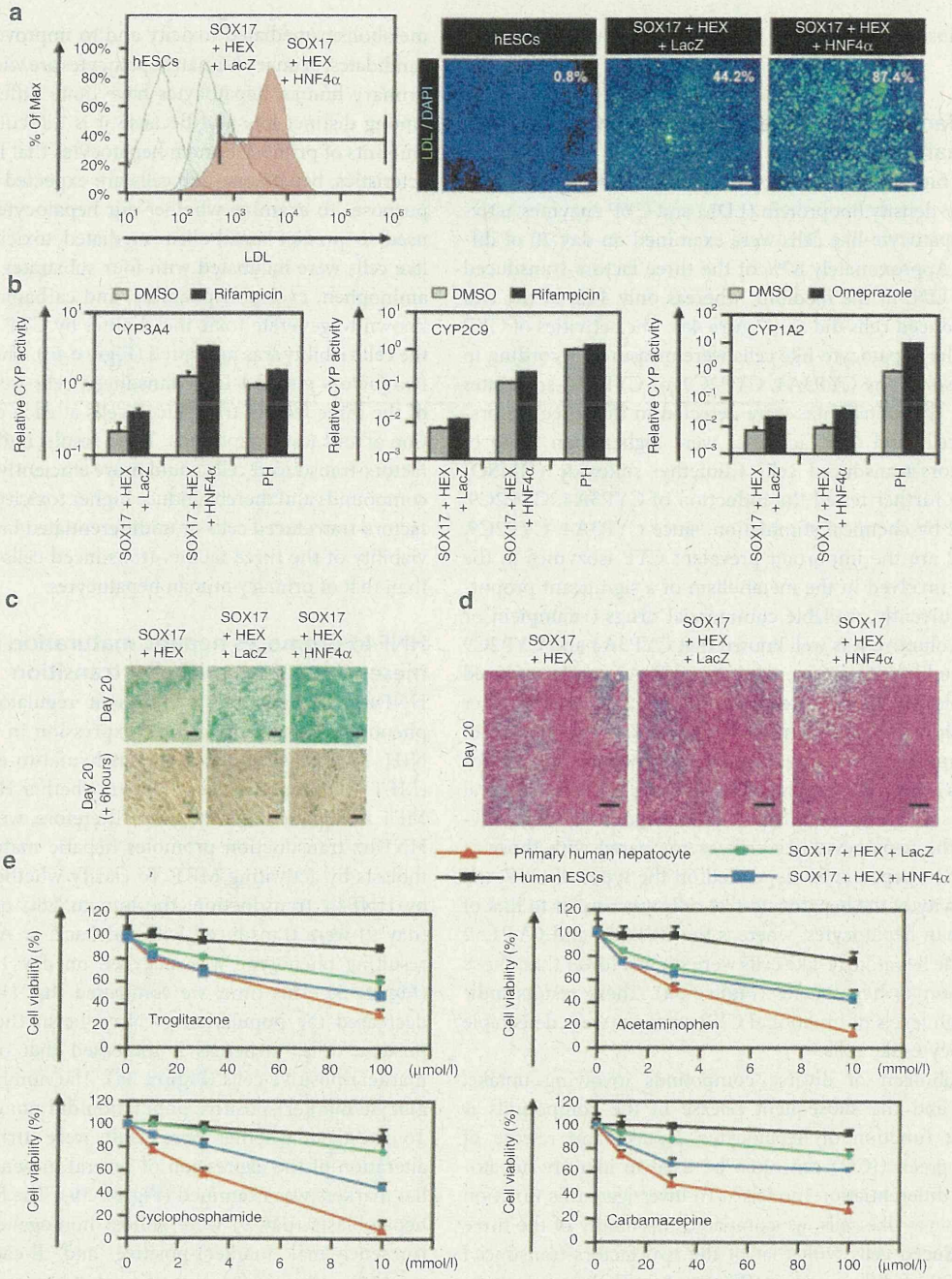

Figure 4 Transduction of the three factors enhances hepatic functions. The human ESCs were differentiated into hepatoblasts and transduced with 3,000 VP/cell of Ad-LacZ or Ad-HNF4α for 1.5 hours and cultured until day 20 of differentiation according to the protocol described in **Figure 2a**. The hepatic functions of the two factors plus Ad-LacZ-transduced cells (SOX17+HEX+LacZ) and the three factors-transduced cells (SOX17+HEX+HNF4α) were compared. (**a**) Undifferentiated human ESCs (hESCs) and the hepatocyte-like cells (day 20) were cultured with medium containing Alexa-Flour 488-labeled LDL (green) for 1 hour, and immunohistochemistry and flow cytometry analysis were performed. The percentage of LDL-positive cells was measured by flow cytometry. Nuclei were counterstained with DAPI (blue). The bar represents 100 μm. (**b**) Induction of CYP3A4 (left), CYP2C9 (middle), or CYP1A2 (right) by DMSO (gray bar), rifampicin (black bar), or omeprazole (black bar) in the hepatocyte-like cells (day 20) and primary human hepatocytes (PH), which were cultured for 48 hours after the cells were plated. On the y-axis, the activity of primary human hepatocytes that have been cultured with medium containing DMSO was taken as 1.0. (**c**) The hepatocyte-like cells (day 20) (upper column) were examined for their ability to take up Indocyanin Green (ICG) and release it 6 hours thereafter (lower column). (**d**) Glycogen storage of the hepatocyte-like cells (day 20) was assessed by Periodic Acid-Schiff (PAS) staining. PAS staining was performed on day 20 of differentiation. Glycogen storage is indicated by pink or dark red-purple cytoplasms. The bar represents 100 μm. (**e**) The cell viability of undifferentiated human ESCs (black), two factors plus Ad-LacZ-tansduced cells (green), the three factors-transduced cells (blue), and primary human hepatocytes (red) was assessed by Alamar Blue assay after 48 hours exposure to different concentrations of four test compounds (troglitazone, acetaminophen, cyclophosphamide, and carbamazepine). The cell viability is expressed as a percentage of cells treated with solvent only treat: 0.1% DMSO except for carbamazepine: 0.5% DMSO. All data are represented as means ± SD (n = 3). ESC, embryonic stem cell; DMSO, dimethyl sulfoxide; LDL, low-density lipoprotein.

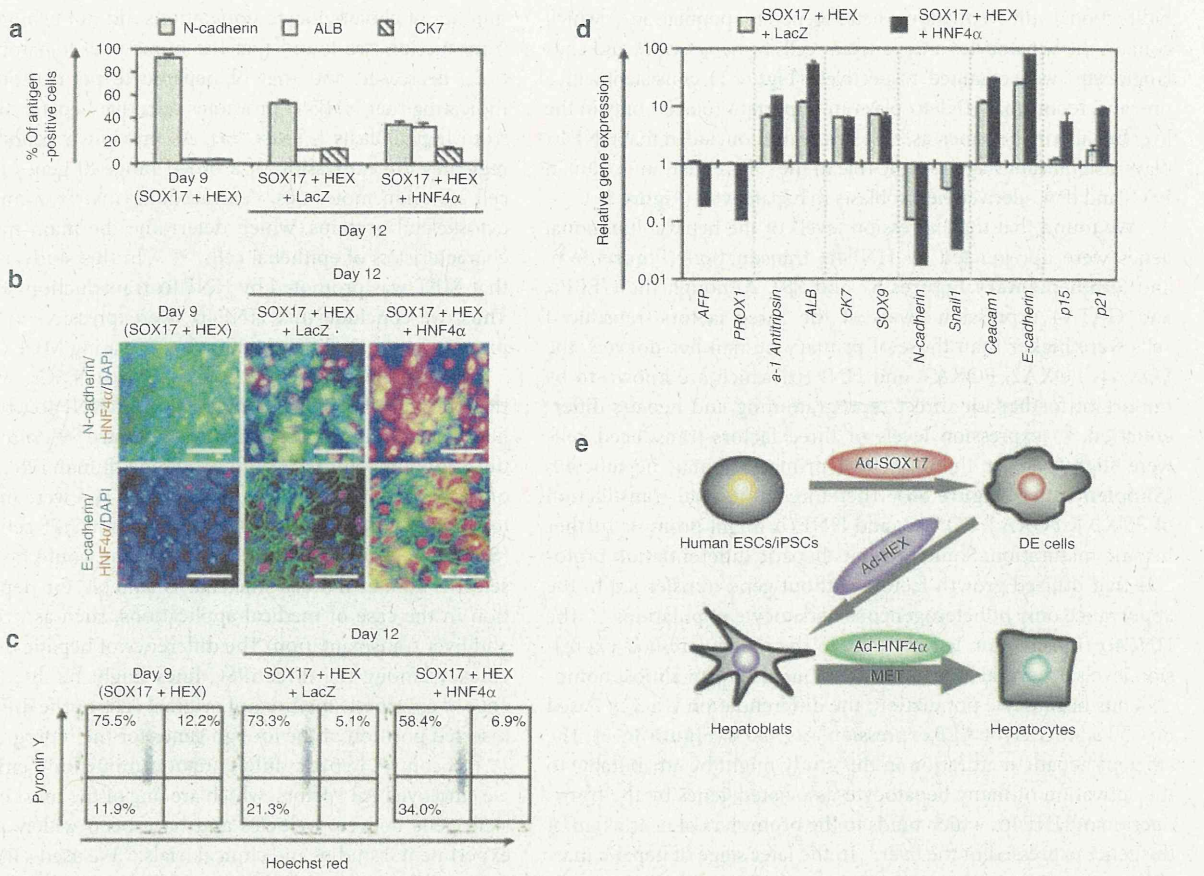

Figure 5 HNF4α promotes hepatic differentiation by activating MET. Human ESCs were differentiated into hepatoblasts according to the protocol described in **Figure 2a**, and then transduced with 3,000 VP/cell of Ad-LacZ or Ad-HNF4α for 1.5 hours, and finally cultured until day 12 of differentiation. (**a**) The hepatoblasts, two factors plus Ad-LacZ-transduced cells (SOX17+HEX+LacZ) (day 12), and the three factors-transduced cells (SOX17+HEX+HNF4α) (day 12) were subjected to immunostaining with anti-N-cadherin, ALB, or CK7 antibodies. The percentage of antigen-positive cells was measured by flow cytometry. (**b**) The cells were subjected to immunostaining with anti-N-cadherin (green), E-cadherin (green), or HNF4α (red) antibodies on day 9 or day 12 of differentiation. Nuclei were counterstained with DAPI (blue). The bar represents 50 μm. Similar results were obtained in two independent experiments. (**c**) The cell cycle was examined on day 9 or day 12 of differentiation. The cells were stained with Pyronin Y (y-axis) and Hoechst 33342 (x-axis) and then analyzed by flow cytometry. The growth fraction of cells is the population of actively dividing cells (G1/S/G2/M). (**d**) The expression levels of *AFP*, *PROX1*, *α-1-antitrypsin*, *ALB*, *CK7*, *SOX9*, *N-cadherin*, *Snail1*, *Ceacam1*, *E-cadherin*, *p15*, and *p21* were examined by real-time RT-PCR on day 9 or day 12 of differentiation. The expression level of hepatoblasts (day 9) was taken as 1.0. All data are represented as means ± SD ($n = 3$). (**e**) The model of efficient hepatic differentiation from human ESCs and iPSCs in this study is summarized. The human ESCs and iPSCs differentiate into hepatocytes via definitive endoderm and hepatoblasts. At each stage, the differentiation is promoted by stage-specific transduction of appropriate functional genes. In the last stage of hepatic differentiation, HNF4α transduction provokes hepatic maturation by activating MET. ESC, embryonic stem cell; HNF4α, hepatocyte nuclear factor 4α; iPSC, induced pluripotent stem cell; MET, mesenchymal-to-epithelial transition; RT-PCR, reverse transcription-PCR; VP, vector particle.

The gene expression levels of hepatocyte markers (*α-1-antitrypsin* and *ALB*)[20] and epithelial markers (*Ceacam1* and *E-cadherin*) were upregulated by HNF4α transduction. On the other hand, the gene expression levels of hepatoblast markers (*AFP* and *PROX1*)[31], mesenchymal markers (*N-cadherin* and *Snail*)[32], and cyclin dependent kinase inhibitor (*p15* and *p21*)[33] were downregulated by HNF4α transduction. HNF4α transduction did not change the expression levels of cholangiocyte markers (*CK7* and *SOX9*). We conclude that HNF4α promotes hepatic maturation by activating MET.

DISCUSSION

This study has two main purposes: the generation of functional hepatocytes from human ESCs and iPSCs for application to drug toxicity screening in the early phase of pharmaceutical development and; elucidation of the HNF4α function in hepatic maturation from human ESCs. We initially confirmed the importance of transcription factor HNF4α in hepatic differentiation from human ESCs by using a published data set of gene array analysis (**Supplementary Figure S1**).[34] We speculated that HNF4α transduction could enhance hepatic differentiation from human ESCs and iPSCs.

To generate functional hepatocytes from human ESCs and iPSCs and to elucidate the function of HNF4α in hepatic differentiation from human ESCs, we examined the stage-specific roles of HNF4α. We found that hepatoblast (day 9) stage-specific HNF4α transduction promoted hepatic differentiation (**Figure 1**). Because endogenous HNF4α is initially expressed in the hepatoblast,[9,10] our system might adequately reflect early embryogenesis. However, HNF4α transduction at an inappropriate stage (day 6 or day 12) promoted

bidirectional differentiation; heterogeneous populations, which contain the hepatocytes and pancreas cells or hepatocytes and cholangiocytes, were obtained, respectively (**Figure 1**), consistent with a previous report that HNF4α plays an important role not only in the liver but also in the pancreas.[12] Therefore, we concluded that HNF4α plays a significant stage-specific role in the differentiation of human ESC- and iPSC-derived hepatoblasts to hepatocytes (**Figure 5e**).

We found that the expression levels of the hepatic functional genes were upregulated by HNF4α transduction (**Figure 3a,b**, and **Supplementary Figures S7** and **S8**). Although the c/EBPα and GATA4 expression levels of the three factors-transduced cells were higher than those of primary human hepatocytes, the FOXA1, FOXA2, FOXA3, and HNF1α, which are known to be important for hepatic direct reprogramming and hepatic differentiation,[35,36] expression levels of three factors-transduced cells were slightly lower than those of primary human hepatocytes (**Supplementary Figure S8**). Therefore, additional transduction of FOXA1, FOXA2, FOXA3, and HNF1α might promote further hepatic maturation. Some previous hepatic differentiation protocols that utilized growth factors without gene transfer led to the appearance only of heterogeneous hepatocyte populations.[4–6] The HNF4α transduction led not only to the upregulation of expression levels of several hepatic markers but also to an almost homogeneous hepatocyte population; the differentiation efficacy based on CYPs, ASGR1, or ALB expression was ~80% (**Figure 3c–e**). The efficient hepatic maturation in this study might be attributable to the activation of many hepatocyte-associated genes by the transduction of HNF4α, which binds to the promoters of nearly half of the genes expressed in the liver.[12] In the later stage of hepatic maturation, hepatocyte-associated genes would be strongly upregulated by endogenous transcription factors but not exogenous HNF4α because transgene expression by Ad vectors was almost disappeared on day 18 (**Supplementary Figure S5**). Another reason for the efficient hepatic maturation would be that sequential transduction of SOX17, HEX, and HNF4α could mimic hepatic differentiation in early embryogenesis.

Next, we examined whether or not the hepatocyte-like cells had hepatic functions. The activity of many kinds of CYPs was upregulated by HNF4α transduction (**Figure 4b**). Ad-HNF4α-transduced cells exhibit many characteristics of hepatocytes: uptake of LDL, uptake and excretion of ICG, and storage of glycogen (**Figure 4a,c,d**). Many conventional tests of hepatic characteristics have shown that the hepatocyte-like cells have mature hepatocyte functions. Furthermore, the hepatocyte-like cells can catalyze the toxication of several compounds (**Figure 4e**). Although the activities to catalyze the toxication of test compounds in primary human hepatocytes are slightly higher than those in the hepatocyte-like cells, the handling of primary human hepatocytes is difficult for a number of reasons: since their source is limited, large-scale primary human hepatocytes are difficult to prepare as a homogeneous population. Therefore, the hepatocyte-like cells derived from human ESCs and iPSCs would be a valuable tool for predicting drug toxicity. To utilize the hepatocyte-like cells in a drug toxicity study, further investigation of the drug metabolism capacity and CYP induction potency will be needed.

We also investigated the mechanisms underlying efficient hepatic maturation by HNF4α transduction. Although the number of cholangiocyte populations did not change by HNF4α transduction, we found that the number of hepatoblast populations decreased and that of hepatocyte populations increased, indicating that HNF4α promotes selective hepatic differentiation from hepatoblasts (**Figure 5a**). As previously reported, HNF4α regulates the expression of a broad range of genes that code for cell adhesion molecules,[13] extracellular matrix components, and cytoskeletal proteins, which determine the main morphological characteristics of epithelial cells.[14,35,37] In this study, we elucidated that MET was promoted by HNF4α transduction (**Figure 5b,d**). Thus, we conclude that HNF4α overexpression in hepatoblasts promotes hepatic differentiation by activating MET (**Figure 5e**).

Using human iPSCs as well as human ESCs, we confirmed that the stage-specific overexpression of HNF4α could promote hepatic maturation (**Supplementary Figure S9**). Interestingly, the differentiation efficacies differed among human iPS cell lines: two of the human iPS cell lines (Dotcom and Tic) were more committed to the hepatic lineage than another human iPS cell line (201B7) (**Supplementary Figure S7**). Therefore, it would be necessary to select a human iPS cell line that is suitable for hepatic maturation in the case of medical applications, such as drug screening and liver transplantation. The difference of hepatic differentiation efficacy among the three iPSC lines might be due to the difference of epigenetic memory of original cells or the difference of the inserted position of the foreign genes for the reprogramming.

To control hepatic differentiation mimicking embryogenesis, we employed Ad vectors, which are one of the most efficient transient gene delivery vehicles and have been widely used in both experimental studies and clinical trials.[38] We used a fiber-modified Ad vector containing the EF-1α promoter and a stretch of lysine residue (KKKKKKK, K7) peptides in the C-terminal region of the fiber knob.[19] The K7 peptide targets heparan sulfates on the cellular surface, and the fiber-modified Ad vector containing the K7 peptides was shown to be efficient for transduction into many kinds of cells including human ESCs and human ESC-derived cells.[7–8,19] Thus, Ad vector-mediated transient gene transfer should be a powerful tool for regulating cellular differentiation.

In summary, the findings described here demonstrate that transcription factor HNF4α plays a crucial role in the hepatic differentiation from human ESC-derived hepatoblasts by activating MET (**Figure 5e**). In the present study, both human ESCs and iPSCs (three lines) were used and all cell lines showed efficient hepatic maturation, indicating that our protocol would be a universal tool for cell line-independent differentiation into functional hepatocytes. Moreover, the hepatocyte-like cells can catalyze the toxication of several compounds as primary human hepatocytes. Therefore, our technology, by sequential transduction of SOX17, HEX, and HNF4α, would be a valuable tool for the efficient generation of functional hepatocytes derived from human ESCs and iPSCs, and the hepatocyte-like cells could be used for the prediction of drug toxicity.

MATERIALS AND METHODS

Human ESC and iPSC culture. A human ES cell line, H9 (WiCell Research Institute, Madison, HI), was maintained on a feeder layer of mitomycin C-treated mouse embryonic fibroblasts (Millipore, Billerica, MA) with Repro Stem (Repro CELL, Tokyo, Japan) supplemented with 5 ng/ml fibroblast

growth factor 2 (FGF2) (Sigma, St Louis, MO). Human ESCs were dissociated with 0.1 mg/ml dispase (Roche Diagnostics, Indianapolis, IN) into small clumps and then were subcultured every 4 or 5 days. H9 was used following the Guidelines for Derivation and Utilization of Human Embryonic Stem Cells of the Ministry of Education, Culture, Sports, Science and Technology of Japan. Two human iPS cell lines generated from the human embryonic lung fibroblast cell line MCR5 were provided from the JCRB Cell Bank (Tic, JCRB Number: JCRB1331; and Dotcom, JCRB Number: JCRB1327).[39,40] These human iPS cell lines were maintained on a feeder layer of mitomycin C-treated mouse embryonic fibroblasts with iPSellon (Cardio, Kobe, Japan) supplemented with 10 ng/ml FGF2. Another human iPS cell line, 201B7, generated from human dermal fibroblasts was kindly provided by Dr S. Yamanaka (Kyoto University).[2] The human iPS cell line 201B7 was maintained on a feeder layer of mitomycin C-treated mouse embryonic fibroblasts with Repro Stem (Repro CELL) supplemented with 5 ng/ml FGF2 (Sigma). Human iPSCs were dissociated with 0.1 mg/ml dispase (Roche Diagnostics) into small clumps and were then subcultured every 5 or 6 days.

In vitro *differentiation.* Before the initiation of cellular differentiation, the medium of human ESCs and iPSCs was exchanged for a defined serum-free medium, hESF9, and cultured as we previously reported.[41] hESF9 consists of hESF-GRO medium (Cell Science & Technology Institute, Sendai, Japan) supplemented with 10 μg/ml human recombinant insulin, 5 μg/ml human apotransferrin, 10 μmol/l 2-mercaptoethanol, 10 μmol/l ethanolamine, 10 μmol/l sodium selenite, oleic acid conjugated with fatty-acid-free bovine albumin (BSA), 10 ng/ml FGF2, and 100 ng/ml heparin (all from Sigma).

The differentiation protocol for the induction of DE cells, hepatoblasts, and hepatocytes was based on our previous report with some modifications.[7] Briefly, in mesendoderm differentiation, human ESCs and iPSCs were dissociated into single cells and cultured for 3 days on Matrigel (Becton, Dickinson and Company, Tokyo, Japan) in hESF-DIF medium (Cell Science & Technology Institute) supplemented with 10 μg/ml human recombinant insulin, 5 μg/ml human apotransferrin, 10 μmol/l 2-mercaptoethanol, 10 μmol/l ethanolamine, 10 μmol/l sodium selenite, 0.5 mg/ml BSA, and 100 ng/ml Activin A (R&D Systems, Minneapolis, MN). To generate mesendoderm cells and DE cells, human ESC-derived cells were transduced with 3,000 vector particles (VP)/cell of Ad-SOX17 for 1.5 hours on day 3 and cultured until day 6 on Matrigel (BD) in hESF-DIF medium (Cell Science & Technology Institute) supplemented with 10 μg/ml human recombinant insulin, 5 μg/ml human apotransferrin, 10 μmol/l 2-mercaptoethanol, 10 μmol/l ethanolamine, 10 μmol/l sodium selenite, 0.5 mg/ml BSA, and 100 ng/ml Activin A (R&D Systems). For induction of hepatoblasts, the DE cells were transduced with 3,000 VP/cell of Ad-HEX for 1.5 hours on day 6 and cultured for 3 days on a Matrigel (BD) in hESF-DIF (Cell Science & Technology Institute) medium supplemented with the 10 μg/ml human recombinant insulin, 5 μg/ml human apotransferrin, 10 μmol/l 2-mercaptoethanol, 10 μmol/l ethanolamine, 10 μmol/l sodium selenite, 0.5 mg/ml BSA, 20 ng/ml bone morphogenetic protein 4 (R&D Systems), and 20 ng/ml FGF4 (R&D Systems). In hepatic differentiation, hepatoblasts were transduced with 3,000 VP/cell of Ad-LacZ or Ad-HNF4α for 1.5 hr on day 9 and were cultured for 11 days on Matrigel (BD) in L15 medium (Invitrogen, Carlsbad, CA) supplemented with 8.3% tryptose phosphate broth (BD), 8.3% fetal bovine serum (Vita, Chiba, Japan), 10 μmol/l hydrocortisone 21-hemisuccinate (Sigma), 1 μmol/l insulin, 25 mmol/l $NaHCO_3$ (Wako, Osaka, Japan), 20 ng/ml hepatocyte growth factor (R&D Systems), 20 ng/ml Oncostatin M (R&D Systems), and 10^{-6} mol/l Dexamethasone (Sigma).

Ad vectors. Ad vectors were constructed by an improved *in vitro* ligation method.[42,43] The human HNF4α gene (accession number NM_000457) was amplified by PCR using primers designed to incorporate the 5′ Not I and 3′ Xba I restriction enzyme sites: Fwd 5′-ggcctctagatggaggcagggagaatg-3′ and Rev 5′-ccccgcggccgcagcggcttgctagataac-3′. The human HNF4α gene was inserted into pBSKII (Invitrogen), resulting in pBSKII-HNF4α, and then the human HNF4α gene was inserted into pHMEF5,[44] which contains the human elongation factor-1α (EF-1α) promoter, resulting in pHMEF-HNF4α. The pHMEF-HNF4α was digested with I-CeuI/PI-SceI and ligated into I-Ceu I/PI-SceI-digested pAdHM41-K7,[19] resulting in pAd-HNF4α. The human EF-1α promoter-driven LacZ-, SOX17-, or HEX-expressing Ad vectors, Ad-LacZ, Ad-SOX17, or Ad-HEX, were constructed previously.[7,8,45] Ad-LacZ, Ad-SOX17, Ad-HEX, and Ad-HNF4α, each of which contains a stretch of lysine residue (K7) peptides in the C-terminal region of the fiber knob for more efficient transduction of human ESCs, iPSCs, and DE cells, were generated and purified as described previously.[7] The VP titer was determined by using a spectrophotometric method.[46]

LacZ assay. Human ESC- and iPSC-derived cells were transduced with Ad-LacZ at 3,000 VP/cell for 1.5 hours. After culturing for the indicated number of days, 5-bromo-4-chloro-3-indolyl β-D-galactopyranoside (X-Gal) staining was performed as described previously.[44]

Flow cytometry. Single-cell suspensions of human ESCs, iPSCs, and their derivatives were fixed with methanol at 4 °C for 20 minutes and then incubated with the primary antibody, followed by the secondary antibody. Flow cytometry analysis was performed using a FACS LSR Fortessa flow cytometer (BD).

RNA isolation and reverse transcription-PCR. Total RNA was isolated from human ESCs, iPSCs, and their derivatives using ISOGENE (Nippon Gene) according to the manufacturer's instructions. Primary human hepatocytes were purchased from CellzDirect, Durham, NC. complementary DNA was synthesized using 500 ng of total RNA with a Superscript VILO cDNA synthesis kit (Invitrogen). Real-time reverse transcription-PCR was performed with Taqman gene expression assays (Applied Biosystems, Foster City, CA) or SYBR Premix Ex Taq (TaKaRa) using an ABI PRISM 7000 Sequence Detector (Applied Biosystems). Relative quantification was performed against a standard curve and the values were normalized against the input determined for the housekeeping gene, glyceraldehyde 3-phosphate dehydrogenase. The primer sequences used in this study are described in **Supplementary Table S1**.

Immunohistochemistry. The cells were fixed with methanol or 4% paraformaldehyde (Wako). After blocking with phosphate-buffered saline containing 2% BSA (Sigma) and 0.2% Triton X-100 (Sigma), the cells were incubated with primary antibody at 4 °C for 16 hours, followed by incubation with a secondary antibody that was labeled with Alexa Fluor 488 (Invitrogen) or Alexa Fluor 594 (Invitrogen) at room temperature for 1 hour. All the antibodies are listed in **Supplementary Table S2**.

Assay for CYP activity. To measure cytochrome P450 3A4, 2C9, and 1A2 activity, we performed Lytic assays by using a P450-GloTM CYP3A4 Assay Kit (Promega, Madison, WI). For the CYP3A4 and 2C9 activity assay, undifferentiated human ESCs, the hepatocyte-like cells, and primary human hepatocytes were treated with rifampicin (Sigma), which is the substrate for CYP3A4 and CYP2C9, at a final concentration of 25 μmol/l or DMSO (0.1%) for 48 hours. For the CYP1A2 activity assay, undifferentiated human ESCs, the hepatocyte-like cells, and primary human hepatocytes were treated with omeprazole (Sigma), which is the substrate for CYP1A2, at a final concentration of 10 μM or DMSO (0.1%) for 48 hours. We measured the fluorescence activity with a luminometer (Lumat LB 9507; Berthold, Oak Ridge, TN) according to the manufacturer's instructions.

Pyronin Y/Hoechst Staining. Human ESC-derived cells were stained with Hoechst33342 (Sigma) and Pyronin Y (PY) (Sigma) in Dulbecco's modified Eagle medium (Wako) supplemented with 0.2 mmol/l HEPES and 5% FCS (Invitrogen). Samples were then placed on ice for 15 minutes, and 7-AAD was added to a final concentration of 0.5 mg/ml for exclusion of dead cells. Fluorescence-activated cell-sorting analysis of these cells was

performed on a FACS LSR Fortessa flow cytometer (Becton Dickinson) equipped with a UV-laser.

Cellular uptake and excretion of ICG. ICG (Sigma) was dissolved in DMSO at 100 mg/ml, then added to a culture medium of the hepatocyte-like cells to a final concentration of 1 mg/ml on day 20 of differentiation. After incubation at 37 °C for 60 minutes, the medium with ICG was discarded and the cells were washed with phosphate-buffered saline. The cellular uptake of ICG was then examined by microscopy. Phosphate-buffered saline was then replaced by the culture medium and the cells were incubated at 37 °C for 6 hours. The excretion of ICG was examined by microscopy.

Periodic Acid-Schiff assay for glycogen. The hepatocyte-like cells were fixed with 4% paraformaldehyde and stained using a Periodic Acid-Schiff staining system (Sigma) on day 20 of differentiation according to the manufacturer's instructions.

Cell viability tests. Cell viability was assessed by Alamar Blue assay kit (Invitrogen). After treatment with test compounds[47–50] (troglitazone, acetaminophen, cyclophosphamide, and carbamazepine) (all from Wako) for 2 days, the culture medium was replaced with 0.5 mg/ml solution of Alamar Blue in culturing medium and cells were incubated for 3 hours at 37 °C. The supernatants of the cells were measured at a wavelength of 570 nm with background subtraction at 600 nm in a plate reader. Control refers to incubations in the absence of test compounds and was considered as 100% viability value.

Uptake of LDL. The hepatocyte-like cells were cultured with medium containing Alexa-488-labeled LDL (Invitrogen) for 1 hour, and then the cells that could uptake LDL were assessed by immunohistochemistry and flow cytometry.

Primary human hepatocytes. Cryopreserved human hepatocytes were purchased from CellzDirect (lot Hu8072). The vials of hepatocytes were rapidly thawed in a shaking water bath at 37 °C; the contents of the vial were emptied into prewarmed Cryopreserved Hepatocyte Recovery Medium (CellzDirect) and the suspension was centrifuged at 100*g* for 10 minutes at room temperature. The hepatocytes were seeded at 1.25×10^5 cells/cm^2 in hepatocyte culture medium (Lonza, Walkersville, MD) containing 10% FCS (GIBCO-BRL) onto type I collagen-coated 12-well plates. The medium was replaced with hepatocyte culture medium containing 10% FCS (GIBCO-BRL) 6 hours after seeding. The hepatocytes, which were cultured 48 hours after plating the cells, were used in the experiments.

SUPPLEMENTARY MATERIAL

Figure S1. Genome-wide screening of transcription factors involved in hepatic differentiation emphasizes the importance of the transcription factor HNF4α.
Figure S2. Summary of specific markers for DE cells, hepatoblasts, hepatocytes, cholangiocytes, and pancreas cells.
Figure S3. The formation of DE cells, hepatoblasts, hepatocytes, and cholangiocytes from human ESCs.
Figure S4. Overexpression of HNF4α mRNA in hepatoblasts by Ad-HNF4α transduction.
Figure S5. Time course of LacZ expression in hepatoblasts transduced with Ad-LacZ.
Figure S6. The morphology of the hepatocyte-like cells.
Figure S7. Upregulation of the expression levels of conjugating enzymes and hepatic transporters by HNF4α transduction.
Figure S8. Upregulation of the expression levels of hepatic transcription factors by HNF4α transduction.
Figure S9. Generation of hepatocytes from various human ES or iPS cell lines.
Figure S10. Promotion of MET by HNF4α transduction.
Figure S11. Arrest of cell growth by HNF4α transduction.
Table S1. List of Taqman probes and primers used in this study.
Table S2. List of antibodies used in this study.

ACKNOWLEDGMENTS

We thank Hiroko Matsumura and Misae Nishijima for their excellent technical support. H.M., M.K.F., and T.H. were supported by grants from the Ministry of Health, Labor, and Welfare of Japan. H.M. was also supported by Japan Research foundation For Clinical Phamacology, The Nakatomi Foundation, and The Uehara Memorial Foundation. K.K. (K. Kawabata) was supported by grants from the Ministry of Education, Sports, Science and Technology of Japan (20200076) and the Ministry of Health, Labor, and Welfare of Japan. K.K. (K. Katayama) and F.S. was supported by Program for Promotion of Fundamental Studies in Health Sciences of the National Institute of Biomedical Innovation (NIBIO).

REFERENCES

1. Thomson, JA, Itskovitz-Eldor, J, Shapiro, SS, Waknitz, MA, Swiergiel, JJ, Marshall, VS *et al.* (1998). Embryonic stem cell lines derived from human blastocysts. *Science* **282**: 1145–1147.
2. Takahashi, K, Tanabe, K, Ohnuki, M, Narita, M, Ichisaka, T, Tomoda, K *et al.* (2007). Induction of pluripotent stem cells from adult human fibroblasts by defined factors. *Cell* **131**: 861–872.
3. Murry, CE and Keller, G (2008). Differentiation of embryonic stem cells to clinically relevant populations: lessons from embryonic development. *Cell* **132**: 661–680.
4. Basma, H, Soto-Gutiérrez, A, Yannam, GR, Liu, L, Ito, R, Yamamoto, T *et al.* (2009). Differentiation and transplantation of human embryonic stem cell-derived hepatocytes. *Gastroenterology* **136**: 990–999.
5. Touboul, T, Hannan, NR, Corbineau, S, Martinez, A, Martinet, C, Branchereau, S *et al.* (2010). Generation of functional hepatocytes from human embryonic stem cells under chemically defined conditions that recapitulate liver development. *Hepatology* **51**: 1754–1765.
6. Duan, Y, Ma, X, Ma, X, Zou, W, Wang, C, Bahbahan, IS *et al.* (2010). Differentiation and characterization of metabolically functioning hepatocytes from human embryonic stem cells. *Stem Cells* **28**: 674–686.
7. Inamura, M, Kawabata, K, Takayama, K, Tashiro, K, Sakurai, F, Katayama, K *et al.* (2011). Efficient generation of hepatoblasts from human ES cells and iPS cells by transient overexpression of homeobox gene HEX. *Mol Ther* **19**: 400–407.
8. Takayama, K, Inamura, M, Kawabata, K, Tashiro, K, Katayama, K, Sakurai, F *et al.* (2011). Efficient and directive generation of two distinct endoderm lineages from human ESCs and iPSCs by differentiation stage-specific SOX17 transduction. *PLoS ONE* **6**: e21780.
9. Duncan, SA, Manova, K, Chen, WS, Hoodless, P, Weinstein, DC, Bachvarova, RF *et al.* (1994). Expression of transcription factor HNF-4 in the extraembryonic endoderm, gut, and nephrogenic tissue of the developing mouse embryo: HNF-4 is a marker for primary endoderm in the implanting blastocyst. *Proc Natl Acad Sci USA* **91**: 7598–7602.
10. Taraviras, S, Monaghan, AP, Schütz, G and Kelsey, G (1994). Characterization of the mouse HNF-4 gene and its expression during mouse embryogenesis. *Mech Dev* **48**: 67–79.
11. Parviz, F, Matullo, C, Garrison, WD, Savatski, L, Adamson, JW, Ning, G *et al.* (2003). Hepatocyte nuclear factor 4alpha controls the development of a hepatic epithelium and liver morphogenesis. *Nat Genet* **34**: 292–296.
12. Odom, DT, Zizlsperger, N, Gordon, DB, Bell, GW, Rinaldi, NJ, Murray, HL *et al.* (2004). Control of pancreas and liver gene expression by HNF transcription factors. *Science* **303**: 1378–1381.
13. Battle, MA, Konopka, G, Parviz, F, Gaggl, AL, Yang, C, Sladek, FM *et al.* (2006). Hepatocyte nuclear factor 4alpha orchestrates expression of cell adhesion proteins during the epithelial transformation of the developing liver. *Proc Natl Acad Sci USA* **103**: 8419–8424.
14. Konopka, G, Tekiela, J, Iverson, M, Wells, C and Duncan, SA (2007). Junctional adhesion molecule-A is critical for the formation of pseudocanaliculi and modulates E-cadherin expression in hepatic cells. *J Biol Chem* **282**: 28137–28148.
15. Li, J, Ning, G and Duncan, SA (2000). Mammalian hepatocyte differentiation requires the transcription factor HNF-4alpha. *Genes Dev* **14**: 464–474.
16. Hayhurst, GP, Lee, YH, Lambert, G, Ward, JM and Gonzalez, FJ (2001). Hepatocyte nuclear factor 4alpha (nuclear receptor 2A1) is essential for maintenance of hepatic gene expression and lipid homeostasis. *Mol Cell Biol* **21**: 1393–1403.
17. Khurana, S, Jaiswal, AK and Mukhopadhyay, A (2010). Hepatocyte nuclear factor-4alpha induces transdifferentiation of hematopoietic cells into hepatocytes. *J Biol Chem* **285**: 4725–4731.
18. Suetsugu, A, Nagaki, M, Aoki, H, Motohashi, T, Kunisada, T and Moriwaki, H (2008). Differentiation of mouse hepatic progenitor cells induced by hepatocyte nuclear factor-4 and cell transplantation in mice with liver fibrosis. *Transplantation* **86**: 1178–1186.
19. Koizumi, N, Mizuguchi, H, Utoguchi, N, Watanabe, Y and Hayakawa, T (2003). Generation of fiber-modified adenovirus vectors containing heterologous peptides in both the HI loop and C terminus of the fiber knob. *J Gene Med* **5**: 267–276.
20. Shiojiri, N (1984). The origin of intrahepatic bile duct cells in the mouse. *J Embryol Exp Morphol* **79**: 25–39.
21. Moll, R, Franke, WW, Schiller, DL, Geiger, B and Krepler, R (1982). The catalog of human cytokeratins: patterns of expression in normal epithelia, tumors and cultured cells. *Cell* **31**: 11–24.

22. Antoniou, A, Raynaud, P, Cordi, S, Zong, Y, Tronche, F, Stanger, BZ *et al.* (2009). Intrahepatic bile ducts develop according to a new mode of tubulogenesis regulated by the transcription factor SOX9. *Gastroenterology* **136**: 2325–2333.
23. Offield, MF, Jetton, TL, Labosky, PA, Ray, M, Stein, RW, Magnuson, MA *et al.* (1996). PDX-1 is required for pancreatic outgrowth and differentiation of the rostral duodenum. *Development* **122**: 983–995.
24. Sussel, L, Kalamaras, J, Hartigan-O'Connor, DJ, Meneses, JJ, Pedersen, RA, Rubenstein, JL *et al.* (1998). Mice lacking the homeodomain transcription factor Nkx2.2 have diabetes due to arrested differentiation of pancreatic beta cells. *Development* **125**: 2213–2221.
25. Ingelman-Sundberg, M, Oscarson, M and McLellan, RA (1999). Polymorphic human cytochrome P450 enzymes: an opportunity for individualized drug treatment. *Trends Pharmacol Sci* **20**: 342–349.
26. Henderson, CJ, Otto, DM, Carrie, D, Magnuson, MA, McLaren, AW, Rosewell, I *et al.* (2003). Inactivation of the hepatic cytochrome P450 system by conditional deletion of hepatic cytochrome P450 reductase. *J Biol Chem* **278**: 13480–13486.
27. Yamada, T, Yoshikawa, M, Kanda, S, Kato, Y, Nakajima, Y, Ishizaka, S *et al.* (2002). *In vitro* differentiation of embryonic stem cells into hepatocyte-like cells identified by cellular uptake of indocyanine green. *Stem Cells* **20**: 146–154.
28. Anzenbacher, P and Anzenbacherová, E (2001). Cytochromes P450 and metabolism of xenobiotics. *Cell Mol Life Sci* **58**: 737–747.
29. Zhao, D, Chen, S, Cai, J, Guo, Y, Song, Z, Che, J *et al.* (2009). Derivation and characterization of hepatic progenitor cells from human embryonic stem cells. *PLoS ONE* **4**: e6468.
30. Hatta, K, Takagi, S, Fujisawa, H and Takeichi, M (1987). Spatial and temporal expression pattern of N-cadherin cell adhesion molecules correlated with morphogenetic processes of chicken embryos. *Dev Biol* **120**: 215–227.
31. Shiojiri, N (1981). Enzymo- and immunocytochemical analyses of the differentiation of liver cells in the prenatal mouse. *J Embryol Exp Morphol* **62**: 139–152.
32. Lee, JM, Dedhar, S, Kalluri, R and Thompson, EW (2006). The epithelial-mesenchymal transition: new insights in signaling, development, and disease. *J Cell Biol* **172**: 973–981.
33. Macleod, KF, Sherry, N, Hannon, G, Beach, D, Tokino, T, Kinzler, K *et al.* (1995). p53-dependent and independent expression of p21 during cell growth, differentiation, and DNA damage. *Genes Dev* **9**: 935–944.
34. Si-Tayeb, K, Noto, FK, Nagaoka, M, Li, J, Battle, MA, Duris, C *et al.* (2010). Highly efficient generation of human hepatocyte-like cells from induced pluripotent stem cells. *Hepatology* **51**: 297–305.
35. Sekiya, S and Suzuki, A (2011). Direct conversion of mouse fibroblasts to hepatocyte-like cells by defined factors. *Nature* **475**: 390–393.
36. Huang, P, He, Z, Ji, S, Sun, H, Xiang, D, Liu, C *et al.* (2011). Induction of functional hepatocyte-like cells from mouse fibroblasts by defined factors. *Nature* **475**: 386–389.
37. Satohisa, S, Chiba, H, Osanai, M, Ohno, S, Kojima, T, Saito, T *et al.* (2005). Behavior of tight-junction, adherens-junction and cell polarity proteins during HNF-4alpha-induced epithelial polarization. *Exp Cell Res* **310**: 66–78.
38. Xu, ZL, Mizuguchi, H, Sakurai, F, Koizumi, N, Hosono, T, Kawabata, K *et al.* (2005). Approaches to improving the kinetics of adenovirus-delivered genes and gene products. *Adv Drug Deliv Rev* **57**: 781–802.
39. Nagata, S, Toyoda, M, Yamaguchi, S, Hirano, K, Makino, H, Nishino, K *et al.* (2009). Efficient reprogramming of human and mouse primary extra-embryonic cells to pluripotent stem cells. *Genes Cells* **14**: 1395–1404.
40. Makino, H, Toyoda, M, Matsumoto, K, Saito, H, Nishino, K, Fukawatase, Y *et al.* (2009). Mesenchymal to embryonic incomplete transition of human cells by chimeric OCT4/3 (POU5F1) with physiological co-activator EWS. *Exp Cell Res* **315**: 2727–2740.
41. Furue, MK, Na, J, Jackson, JP, Okamoto, T, Jones, M, Baker, D *et al.* (2008). Heparin promotes the growth of human embryonic stem cells in a defined serum-free medium. *Proc Natl Acad Sci USA* **105**: 13409–13414.
42. Mizuguchi, H and Kay, MA (1998). Efficient construction of a recombinant adenovirus vector by an improved *in vitro* ligation method. *Hum Gene Ther* **9**: 2577–2583.
43. Mizuguchi, H and Kay, MA (1999). A simple method for constructing E1- and E1/E4-deleted recombinant adenoviral vectors. *Hum Gene Ther* **10**: 2013–2017.
44. Kawabata, K, Sakurai, F, Yamaguchi, T, Hayakawa, T and Mizuguchi, H (2005). Efficient gene transfer into mouse embryonic stem cells with adenovirus vectors. *Mol Ther* **12**: 547–554.
45. Tashiro, K, Kawabata, K, Sakurai, H, Kurachi, S, Sakurai, F, Yamanishi, K *et al.* (2008). Efficient adenovirus vector-mediated PPAR gamma gene transfer into mouse embryoid bodies promotes adipocyte differentiation. *J Gene Med* **10**: 498–507.
46. Maizel, JV Jr, White, DO and Scharff, MD (1968). The polypeptides of adenovirus. I. Evidence for multiple protein components in the virion and a comparison of types 2, 7A, and 12. *Virology* **36**: 115–125.
47. Smith, MT (2003). Mechanisms of troglitazone hepatotoxicity. *Chem Res Toxicol* **16**: 679–687.
48. Dai, Y and Cederbaum, AI (1995). Cytotoxicity of acetaminophen in human cytochrome P4502E1-transfected HepG2 cells. *J Pharmacol Exp Ther* **273**: 1497–1505.
49. Chang, TK, Weber, GF, Crespi, CL and Waxman, DJ (1993). Differential activation of cyclophosphamide and ifosphamide by cytochromes P-450 2B and 3A in human liver microsomes. *Cancer Res* **53**: 5629–5637.
50. Miao, XS and Metcalfe, CD (2003). Determination of carbamazepine and its metabolites in aqueous samples using liquid chromatography-electrospray tandem mass spectrometry. *Anal Chem* **75**: 3731–3738.

THE JOURNAL OF BIOLOGICAL CHEMISTRY VOL. 286, NO. 25, pp. 22403–22413, June 24, 2011

Dendritic Cell-specific Intercellular Adhesion Molecule 3-grabbing Non-integrin (DC-SIGN) Recognizes a Novel Ligand, Mac-2-binding Protein, Characteristically Expressed on Human Colorectal Carcinomas*

Received for publication, December 22, 2010, and in revised form, March 24, 2011 Published, JBC Papers in Press, April 22, 2011, DOI 10.1074/jbc.M110.215301

Motohiro Nonaka[‡1], Bruce Yong Ma[‡§¶2], Hirotsugu Imaeda[‖], Keiko Kawabe[‡], Nobuko Kawasaki[‡], Keiko Hodohara[‖], Nana Kawasaki[**], Akira Andoh[‡‡], Yoshihide Fujiyama[‖], and Toshisuke Kawasaki[‡3]

From the [‡]Research Center for Glycobiotechnology, Ritsumeikan University, Shiga 525-0058, [‖]Department of Medicine, and [‡‡]Division of Mucosal Immunology, Graduate School of Medicine, Shiga University of Medical Science, Shiga 520-2192, [**]Division of Biological Chemistry and Biologicals, National Institute of Health Sciences, Tokyo 158-8501, [§]Department of Computer Science and Systems Engineering, Muroran Institute of Technology, Hokkaido 050-8585, Japan, and [¶]School of Pharmaceutical Engineering and Life Science, Changzhou University, Jiangsu 213164, China

Dendritic cell (DC)-specific intercellular adhesion molecule-3-grabbing non-integrin (DC-SIGN) is a type II transmembrane C-type lectin expressed on DCs such as myeloid DCs and monocyte-derived DCs (MoDCs). Recently, we have reported that DC-SIGN interacts with carcinoembryonic antigen (CEA) expressed on colorectal carcinoma cells. CEA is one of the most widely used tumor markers for gastrointestinal cancers such as colorectal cancer. On the other hand, other groups have reported that the level of Mac-2-binding protein (Mac-2BP) increases in patients with pancreatic, breast, and lung cancers, virus infections such as human immunodeficiency virus and hepatitis C virus, and autoimmune diseases. Here, we first identified Mac-2BP expressed on several colorectal carcinoma cell lines as a novel DC-SIGN ligand through affinity chromatography and mass spectrometry. Interestingly, we found that DC-SIGN selectively recognizes Mac-2BP derived from some colorectal carcinomas but not from the other ones. Furthermore, we found that the α1-3,4-fucose moieties of Le glycans expressed on DC-SIGN-binding Mac-2BP were important for recognition. DC-SIGN-dependent cellular interactions between immature MoDCs and colorectal carcinoma cells significantly inhibited MoDC functional maturation, suggesting that Mac-2BP may provide a tolerogenic microenvironment for colorectal carcinoma cells through DC-SIGN-dependent recognition. Importantly, Mac-2BP was detected as a predominant DC-SIGN ligand expressed on some primary colorectal cancer tissues from certain parts of patients in comparison with CEA from other parts, suggesting that DC-SIGN-binding Mac-2BP bearing tumor-associated Le glycans may become a novel potential colorectal cancer biomarker for some patients instead of CEA.

Dendritic cells (DCs)[4] play a critical role in initiating adaptive immunity by uptaking foreign antigens at the periphery, undergoing maturation during migration to lymph nodes and presenting antigen-derived peptides to naïve T cells (1, 2). For effective recognition of antigens, DCs exploit a wide range of pattern recognition receptors such as Toll-like receptors and C-type lectins (3–5). DC-specific intercellular adhesion molecule-3-grabbing non-integrin (DC-SIGN; CD209) is a type II transmembrane C-type lectin expressed on myeloid DCs in the dermis, mucosae, lymph nodes, and monocyte-derived DCs (MoDCs) (6, 7). DC-SIGN binds to "self" glycan ligands found on human cells and to "foreign" glycans of bacterial or parasitic pathogens, and specifically recognizes glycoconjugates containing mannose (Man), fucose (Fuc), and nonsialylated Lewis $(Le)^a/Le^b$ epitope structures in a Ca^{2+}-dependent manner (8). Through recognition of these glycans, DC-SIGN functions as an adhesion receptor and mediates the binding and internalization of foreign pathogens such as viruses (human immunodeficiency virus and hepatitis C virus), yeasts, bacteria (*Mycobacterium tuberculosis*), and parasites (3).

Recently, we and another group (9, 10) found that DC-SIGN recognizes colorectal carcinoma cells through carcinoembryonic antigen (CEA). DC-SIGN-binding CEA contained tumor-associated Le glycans, which were important for cellular interactions between DCs and colorectal carcinoma cells *in situ*. It is evident that the expression of CEA is limited and can be

* This work was supported by Grants-in-aid for Scientific Research B 20370052 (to T. K.) and C 21590543 (to B. Y. M.), for Young Scientists Start-up 20890255 (to M. N.), and for Japan Society for the Promotion of Science (JSPS) Fellows 22-9530 (to M. N.) from JSPS, the Ministry of Education, Culture, Sports, Science, and Technology of Japan, JSPS Core-to-Core Program Strategic Research Networks (17005) from JSPS, and Research Proposal Grants from Japan Foundation for Applied Enzymology (Osaka, Japan; to B. Y. M.).

[1] A JSPS Research Fellow.

[2] To whom correspondence may be addressed: Research Center for Glycobiotechnology, Ritsumeikan University, Noji-Higashi, Kusatsu, Shiga 525-0058, Japan. Tel.: 81-77-561-3444; Fax: 81-77-561-3496; E-mail: bruceyongma@gmail.com.

[3] To whom correspondence may be addressed: Research Center for Glycobiotechnology, Ritsumeikan University, Noji-Higashi, Kusatsu, Shiga 525-0058, Japan. Tel.: 81-77-561-3444; Fax: 81-77-561-3496; E-mail: tkawasak@fc.ritsumei.ac.jp.

[4] The abbreviations used are: DC, dendritic cell; DC-SIGN, DC-specific intercellular adhesion molecule-3-grabbing non-integrin; rhDC-SIGN-Fc, recombinant human DC-SIGN-human IgG-Fc fusion protein; pAb, polyclonal Ab; Mac-2BP, Mac-2-binding protein; CEA, carcinoembryonic antigen; MoDC, monocyte-derived DC; Le, Lewis; PHA, phytohaemagglutinin; AAL, *Aleuria aurantia* agglutinin; PNGase, peptide *N*-glycosidase; M-CSF, macrophage colony-stimulating factor.

detected only in cancer and embryonic tissues. This glycoprotein is one of the most widely used tumor markers for gastrointestinal cancers such as colorectal carcinomas. However, its sensitivity and specificity are not high, particularly for early stages of the disease such as Dukes A or B stages. Based on our studies, we hypothesized that DC-SIGN may also be involved in the recognition of other glycoproteins, as novel potential biomarkers, expressed on colorectal cancers.

In this study, we first identified Mac-2-binding protein (Mac-2BP) expressed on colorectal carcinoma cells as a novel DC-SIGN ligand through affinity chromatography and mass spectrometry. Mac-2BP, also known as 90K or galectin-3BP, is a secretory glycoprotein expressed on various normal epithelial cells and in human bodily fluids. It has been reported that the level of Mac-2BP increases in patients with pancreatic, breast, and lung cancer, virus infections such as acquired immunodeficiency syndrome and hepatitis C, and autoimmune diseases (11). However, most of the immunological significance of Mac-2BP on colorectal carcinomas remains unknown.

In addition, we found that DC-SIGN-dependent cellular interactions between immature MoDCs and colorectal carcinoma cells mainly expressing Mac-2BP were able to significantly inhibit LPS-induced MoDC functional maturation. Furthermore, we also detected Mac-2BP as a predominant DC-SIGN ligand expressed on some primary colorectal cancer tissues from certain parts of patients in comparison with CEA from the other parts. Therefore, we suggest that Mac-2BP carrying fucosylated glycans may become a novel potential colorectal cancer biomarker for some CEA-low or -negative colorectal cancer patients, and the novel function of DC-SIGN may, at least in part, underlie for its potential use as a novel diagnostic sensor for some colorectal cancer patients through recognition of CEA and Mac-2BP.

EXPERIMENTAL PROCEDURES

Reagents and Antibodies—Recombinant human DC-SIGN-human IgG-Fc fusion protein (rhDC-SIGN-Fc), anti-human DC-SIGN mAb, and anti-Mac-2BP polyclonal antibody (pAb) were purchased from R&D Systems (Minneapolis, MN). Anti-Mac-2BP mAb was from Bender Medsystems (Burlingame, CA). Anti-Le^a, Le^b, and CEA mAbs were from Abcam (Cambridge, MA). Anti-human CD83 and CD86 mAbs were from BD Biosciences. Alexa Fluor 488- or 546-conjugated secondary antibodies were from Invitrogen. HRP-conjugated anti-FLAG antibody and Ultrapure lipopolysaccharide from *Escherichia coli* 0111:B4 were from Sigma-Aldrich. Anti-human DC-SIGN pAb (C-20) was from Santa Cruz Biotechnology (Santa Cruz, CA). All chemicals for gel electrophoresis and Western blotting were purchased from Nacalai Tesque, ATTO Corp. (Tokyo, Japan), Bio-Rad, Thermo Fisher Scientific (Waltham, MA), or Invitrogen.

Cell Lines, Cell Culture, and Immature MoDCs and Maturation of Immature MoDCs—Human colon tumor cell lines COLO205 and SW1116 and human hepatoma cell line HLF were cultured as described previously (10). All of the cell lines were obtained from ATCC. DC-SIGN-expressing HLF cells (HLF-DC-SIGN) were generated by transfection of the pcDNA3-DC-SIGN plasmid (10) with Lipofectamine 2000 reagent (Invitrogen), and then selection was performed in complete medium containing 1 mg/ml G418 (Invitrogen) for stable transfectants. Isolation of human peripheral blood mononuclear cells from healthy donors, positive selection of $CD14^+$ cells, induction of immature MoDCs, and maturation of MoDCs were conducted as described previously (10) in accordance with the Declaration of Helsinki. DC maturation was confirmed by expression of CD83, a DC-specific maturation marker, and CD86, a costimulatory molecule, on mature but not immature DCs.

Cellular Adhesion Assay—HLF-DC-SIGN or HLF cells were incubated into confluent culture at 37 °C in 96-well plates and then COLO205 cells, which had been prelabeled with the green fluorescent dye calcein-AM (Invitrogen), were added onto the wells and incubated for 1 h. After unbound cells were removed with wash buffer (0.5% BSA, 150 mM NaCl, 20 mM Tris/HCl (pH 7.5), and 1 mM $CaCl_2$), cells on the plates were lysed with lysis buffer (20 mM Tris/HCl (pH 7.5), and 0.1% SDS) and analyzed by fluorometry at 488 nm. Population of adhered COLO205 cells was calculated as the percentage of maximal binding, which was determined by the lysed total amount of added calcein-AM-labeled cells (100% adhesions).

ELISA Analysis—For analysis of DC-SIGN binding to proteins secreted by HLF, COLO205, or SW1116 cells, culture supernatants were mixed with coating buffer (Na_2CO_3 buffer, pH 9.6) and then coated onto NUNC maxisorp 96-well plates (Nalge Nunc) overnight at 4 °C. Mannan was used as a positive control. Then, the plates were blocked with 3% BSA in coating buffer for 1 h at room temperature, washed with TBS (pH 7.6) containing 0.05% Tween 20, and then incubated with 0.4 μg/ml rhDC-SIGN-FLAG in 1% BSA in TBS (pH 7.6) containing 5 mM $CaCl_2$ for 1 h at room temperature. After the plates had been washed, HRP-conjugated anti-FLAG mAb was added, followed by incubation for 1 h.

For analysis of DC-SIGN binding to Mac-2BP secreted by human hepatoma and colorectal carcinoma cell lines, 1 μg/ml anti-Mac-2BP pAbs were precoated onto 96-well plates overnight at 4 °C. After blocking, culture supernatants of HepG2, HLF, COLO205, LS180, or SW1116 cells were added, followed by incubation for 1 h at room temperature. DC-SIGN binding was assayed using rhDC-SIGN-FLAG, as described above.

For quantitative kinetic data of association between DC-SIGN and Mac-2BP, 5 ng/well of Mac-2BP captured onto plates were reacted for 2 h with different concentrations (0.063–8.000 nM) of rhDC-SIGN-FLAG in the presence of 5 mM $CaCl_2$. Quantitative kinetic data (K_d app and B_{max}) were calculated based on the amounts of total and unbound rhDC-SIGN-FLAG using a nonlinear regression model by GraphPad Prism software (version 4.0c). DC-SIGN was regarded as a tetramer.

For determination of the glycan profile of COLO205-derived Mac-2BP, anti-Mac-2BP pAb was precoated onto 96-well plates overnight at 4 °C. After blocking, culture supernatants of HLF or COLO205 cells were added, followed by incubation for 1 h at room temperature. Then the captured Mac-2BP was incubated with biotin-conjugated plant lectins (phytohemeagglutinin (PHA)-L4, *Lycopersicon esculentum* agglutinin, and *Aleuria aurantia* agglutinin (AAL)), followed by incuba-

tion with HRP-conjugated avidin. After development, binding was quantitated by measuring the absorbance at 450 nm using a Multilabel Counter (PerkinElmer Life Sciences) in accordance with the manufacturer's instructions. All experiments were performed in triplicate and were repeated a minimum of three times.

Preparation of Membrane Fractions, Affinity Chromatography, and Mass Spectrometry—Affinity sepharoses were prepared using Seize X Protein G Immunoprecipitation kit (Thermo Fisher Scientific). According to the manufacturer's instructions, rhDC-SIGN-Fc and hIgG-Fc proteins were immobilized to Protein G-Sepharose using the cross-linker disuccinimidyl suberate. Cells were homogenized in homogenization buffer (10 mM Tris/HCl (pH 7.6), 0.5 mM $MgCl_2$, and protease inhibitor mixture), and then tonicity was restored into 150 mM NaCl. The homogenate was centrifuged at 500 × *g* for 5 min at 4 °C to remove cell debris and nuclei. The supernatant was supplemented with EDTA to 5 mM and then centrifuged at 150,000 × *g* for 45 min at 4 °C. The resulting total membrane pellet was solubilized with lysis buffer (150 mM NaCl, 20 mM Tris/HCl (pH 7.5), 1 mM EDTA, 1% Triton X-100, and protease inhibitor mixture) for 60 min at 4 °C and then centrifuged at 10,000 × *g* for 60 min at 4 °C. The supernatant was saved as the solubilized COLO205 membrane proteins and was applied to a rhDC-SIGN-Fc or hIgG-Fc affinity column. After the column had been washed with TBS buffer (pH 7.5) containing 5 mM $CaCl_2$ and 0.1% Triton X-100, the proteins bound to the column were eluted with TBS buffer (pH 7.5) containing 10 mM EDTA and 0.1% Triton X-100. The EDTA-eluted fractions were buffer-exchanged, applied again to the same column and then eluted with TBS buffer (pH 7.5) containing 50 mM Man. The secondly eluted proteins were resolved on a 5–20% Tris/HCl gradient gel (ATTO Corporation) and then stained with a silver staining kit (Wako Pure Chemical Industries). Bands were excised from the gel and subjected to in-gel digestion. The peptides released from the gel were subjected to LC/MS/MS with a linear ion trap mass spectrometer (LTQ, Thermo Fisher Scientific) interfaced on-line with a nano HPLC (Paradigm, Michrom BioResources, Auburn, CA). The eluents consisted of H_2O containing 2% CH_3CN and 0.1% formic acid (Pump A), and 90% CH_3CN and 0.1% formic acid (Pump B), and the peptides were eluted with a linear gradient of 5–80% from Pump B. Data-dependent MS/MS acquisition was performed for the most intense ions as precursors. Proteins were identified by searching the Swiss-Prot *Homo sapiens* and NCBInr database (human) using the Mascot search engine (Matrixscience, London, UK) and Bioworks search engine (Thermo Fisher Scientific), respectively.

Ligand Precipitation, Immunoprecipitation, and Immunoblotting—Solubilized membrane proteins from HLF, COLO205, and SW1116 cells were prepared as described above, and used as ligand precipitation, immunoprecipitation, and immunoblot samples. To identify the proteins carrying DC-SIGN carbohydrate ligands on colorectal carcinomas, precipitation was performed using rhDC-SIGN-Fc- or rhIgG-Fc-Protein G beads, and the bound proteins were eluted with EDTA as immunoblot samples. The samples were resolved on 5–20% gradient SDS-PAGE gels (ATTO Corp.) and then transferred to nitrocellulose membranes, followed by immunoblot detection with specific antibodies. For visualization, a Super-Signal West Pico Chemiluminescent kit (Thermo Fisher Scientific) was used with HRP-conjugated anti-mouse or anti-goat IgG. The amounts of SDS-PAGE loading proteins from HLF, COLO205, and SW1116 cells were adjusted on the basis of cell numbers, and we confirmed by Bradford method that whole membrane lysates contained 15–20 μg/lane and culture supernatant contained 27–32 μg/lane of comparable proteins (data not shown).

Glycan Digestion Assay—For peptide-*N*-glycosidase (PNGase) F treatment, membrane proteins prepared from COLO205 cells, as described above, were adjusted to 10 mM EDTA, 0.1% SDS, and 0.1% Nonidet P-40 and then incubated overnight with or without PNGase F at 37 °C. After replacement in Hepes buffer (pH 7.5)-0.15 M NaCl by ultrafiltration, DC-SIGN ligands were precipitated with rhDC-SIGN-Fc, followed by SDS-PAGE and immunoblotting with anti-Mac-2BP pAb. For α1-3,4-fucosidase treatment, a membrane pellet of COLO205 cells prepared as described above was suspended in 20 mM KH_2PO_4 (pH 5.0) buffer containing 1% Nonidet P-40, followed by incubation overnight with or without α1-3,4-fucosidase at 37 °C, and then ligand precipitation with rhDC-SIGN-Fc, anti-Le^a or -Le^b mAb, SDS-PAGE, and immunoblotting with anti-Mac-2BP pAb.

MoDC Functional Maturation—To determine the effect of a MoDC-COLO205-cocultured supernatant on LPS-induced functional maturation of MoDCs, immature MoDCs were incubated in a MoDC-cultured or MoDC-SW1116-cocultured supernatant for 3 days in the presence of IL-4 (500 units/ml), GM-CSF (800 units/ml), and LPS (1 ng/ml). Supernatant of MoDC, which cultured in the presence of anti-DC-SIGN pAb, was used as a control. Cultures were replenished with fresh supernatant on the second day. The effect on MoDC functional maturation was determined by cell-surface expression of CD83, a DC-specific maturation marker, and CD86, a costimulatory molecule on mature DCs, using FACS Calibur™, and the mean fluorescent intensity was calculated with CELLQUEST software™ (BD Biosciences). All experiments were performed in triplicate and were repeated a minimum of three times.

Histochemistry—Clinical colorectal cancer tissue specimens were purchased from SuperBioChips Laboratories (Seoul, Korea), or obtained from Shiga University of Medical Science with informed consent. This project was approved by the ethics committee of Shiga University of Medical Science. Following deparaffinization and hydration of paraffin-embedded tissue sections, antigen retrieval was performed by steaming in citrate buffer (pH 6.0). After blocking with 1% BSA, the slides were incubated with 1 μg/ml of anti-Mac-2BP pAb followed by Alexa Fluor 546-conjugated secondary Ab (for anti-Mac-2BP staining), anti-CEA mAb (1:50) followed by Alexa Fluor 488-conjugated secondary Ab (for anti-CEA staining), and/or 1 μg/ml of allophycocyanin-conjugated rhDC-SIGN-FLAG (for direct rhDC-SIGN staining, donor 1) or rhDC-SIGN-FLAG followed by anti-FLAG mAb and Alexa Fluor 488-conjugated secondary Ab (for indirect rhDC-SIGN staining, donor 2), and then washed and mounted. To observe the expression of DC-SIGN ligands on COLO205 cells, cells were stained with 1

μg/ml of rhDC-SIGN-allophycocyanin and anti-Mac-2BP pAb, followed by Alexa Fluor 488-conjugated secondary Ab in the presence of $CaCl_2$ or EDTA. To investigate cellular interactions between immature MoDCs and COLO205 cells, cells were coincubated for 1 h at 37 °C and then stained with 1 μg/ml of anti-DC-SIGN mAb and anti-Mac-2BP pAb or anti-Le^b mAb, followed by Alexa Fluor 488- and 546-conjugated secondary Abs. The cellular interactions were visualized by laser confocal microscopy.

Statistical Analysis—The results are expressed as the means ± S.D. of data obtained in three experiments performed in triplicate. Statistical significance was determined by means of Student's *t* test.

RESULTS

DC-SIGN-mediated Cellular Adhesions and Mac-2BP Identified as a Novel DC-SIGN Ligand on Colorectal Carcinoma Cells—To determine whether or not DC-SIGN-expressing cells interact with human colorectal carcinoma cells, we coincubated either human hepatoma HLF cells or DC-SIGN-expressing HLF (HLF-DC-SIGN) cells with COLO205 cells. As shown in Fig. 1*A*, COLO205 cells significantly bound to HLF-DC-SIGN cells compared with control HLF cells, indicating that DC-SIGN is sufficiently involved in the cellular adhesions through interaction with DC-SIGN ligands expressed on COLO205 cells.

To completely isolate DC-SIGN ligands expressed on COLO205, the ligand glycoproteins from solubilized membrane fractions were purified by an affinity column of recombinant human DC-SIGN-Fc (rhDC-SIGN-Fc) and then analyzed by nano-LC/MS/MS, as described under "Experimental Procedures." The two major silver-stained bands, which were independent of the Fc portion of the DC-SIGN-Fc chimeric protein, indicated by the arrows (Fig. 1*B*) from rhDC-SIGN-Fc column were identified as matured and degraded Mac-2BP, respectively (Fig. 1*C*).

On the other hand, we previously identified CEA as the main DC-SIGN ligand expressed on SW1116 cells, another human colorectal carcinoma cell line. Therefore, we compared the expression levels of Mac-2BP and CEA between COLO205 and SW1116 cells by confocal microscopy. As shown in Fig. 1*D*, the cell-surface expression of Mac-2BP was markedly higher on COLO205 than SW1116 cells. In contrast, CEA could hardly be detected on COLO205 cells compared with its abundant expression on SW1116 cells.

Next, to confirm the interaction of DC-SIGN with Mac-2BP *in vitro*, DC-SIGN ligands purified from COLO205, SW1116, and human hepatoma HLF cells were immunoblotted with anti-Mac-2BP pAb (Fig. 1*E*) or anti-CEA mAb (Fig. 1*F*). The results showed that COLO205-derived Mac-2BP, but not HLF or SW1116-derived Mac-2BP, apparently interacted with rhDC-SIGN (Fig. 1*E*). In contrast, we observed high-level expression of CEA on SW1116 cells and its distinct association with rhDC-SIGN (Fig. 1*F*), whereas we could not detect any association of COLO205-derived CEA with rhDC-SIGN. Confocal microscopy also showed that Mac-2BP (*green*) was substantially colocalized with allophycocyanin-fluoresceinated rhDC-SIGN (*red*) on COLO205 cells in a Ca^{2+}-dependent manner (Fig. 1*G*). These findings indicated that Mac-2BP is a novel DC-SIGN ligand expressed on colorectal carcinoma cells and that DC-SIGN selectively interacts with Mac-2BP expressed on particular carcinoma cells as opposed to CEA.

DC-SIGN Binds to Mac-2BP Secreted by Several Colorectal Carcinoma Cell Lines—Mac-2BP and CEA were known originally as secretory proteins. Therefore, we examined whether or not DC-SIGN ligands existed in COLO205-, SW1116-, or HLF-cultured supernatants. As shown in Fig. 2*A*, ELISA analysis revealed that DC-SIGN ligand glycoproteins could be detected in a Ca^{2+}-dependent manner in both COLO205- and SW1116-cultured supernatants, but not in a HLF-cultured supernatant.

Next, to verify that DC-SIGN interacts with secreted CEA and Mac-2BP, purified DC-SIGN ligands from HLF-, COLO205-, and SW1116-cultured supernatants were immunoblotted with anti-Mac-2BP pAb and anti-CEA mAb, respectively. Interestingly, only Mac-2BP secreted by COLO205 cells, but not by HLF or SW1116 cells, interacted with rhDC-SIGN (Fig. 2*B*). On the other hand, CEA, which can interact with DC-SIGN, was only observed in the SW1116-cultured supernatant (Fig. 2*C*). Moreover, we investigated the interaction of DC-SIGN with Mac-2BP secreted by several other human hepatoma and colorectal carcinoma cell lines (Fig. 2*D*). The ELISA data showed that the human hepatoma HepG2 and HLF, and human colorectal carcinoma COLO205, LS180, and SW1116 cell lines all apparently expressed Mac-2BP (Fig. 2*D*, *upper panel*); however, only the COLO205- and LS180-derived Mac-2BP had the ability to interact with rhDC-SIGN (*lower panel*), indicating that parts of colorectal carcinomas can secrete DC-SIGN-recognizing Mac-2BP. These results also suggest that distinct glycoforms of Mac-2BP exist in different colorectal carcinomas.

DC-SIGN Binds to Mac-2BP from Colorectal Carcinoma Cells in Ca^{2+}-dependent and Dose-dependent Manners—To quantitatively characterize the direct association between DC-SIGN and COLO205-derived Mac-2BP, we performed ELISA experiments. As shown in Fig. 3*A*, the interactions were monitored as the changes in the ELISA responses, and the Ca^{2+} chelator EDTA completely blocked the interactions, suggesting that DC-SIGN directly binds to glycans on Mac-2BP in a dose-dependent manner, and the interaction occurs in a Ca^{2+}-dependent manner and the CRD of DC-SIGN mediates the binding.

Moreover, their affinity level was shown to be extremely high when the apparent dissociation constant (K_d app = 2.50 (±0.66)) was calculated by fitting a curve using nonlinear regression model (Fig. 3*B*). These results suggest the potential physiological interaction between DC-SIGN and Mac-2BP in the colon microenvironment.

DC-SIGN Recognizes Fucose Residues of Le N-Glycans on Mac-2BP from Colorectal Carcinoma Cells—To determine whether or not interaction of Mac-2BP with DC-SIGN is *N*-glycan-dependent, Mac-2BP purified from COLO205 cells was treated with PNGase F and then precipitated with rhDC-SIGN. Fig. 4*A* shows that the Mac-2BP band shifted from 90 to 65 kDa on PNGase F treatment and that the PNGase F-treated form had completely lost the ability to bind rhDC-SIGN, indicating

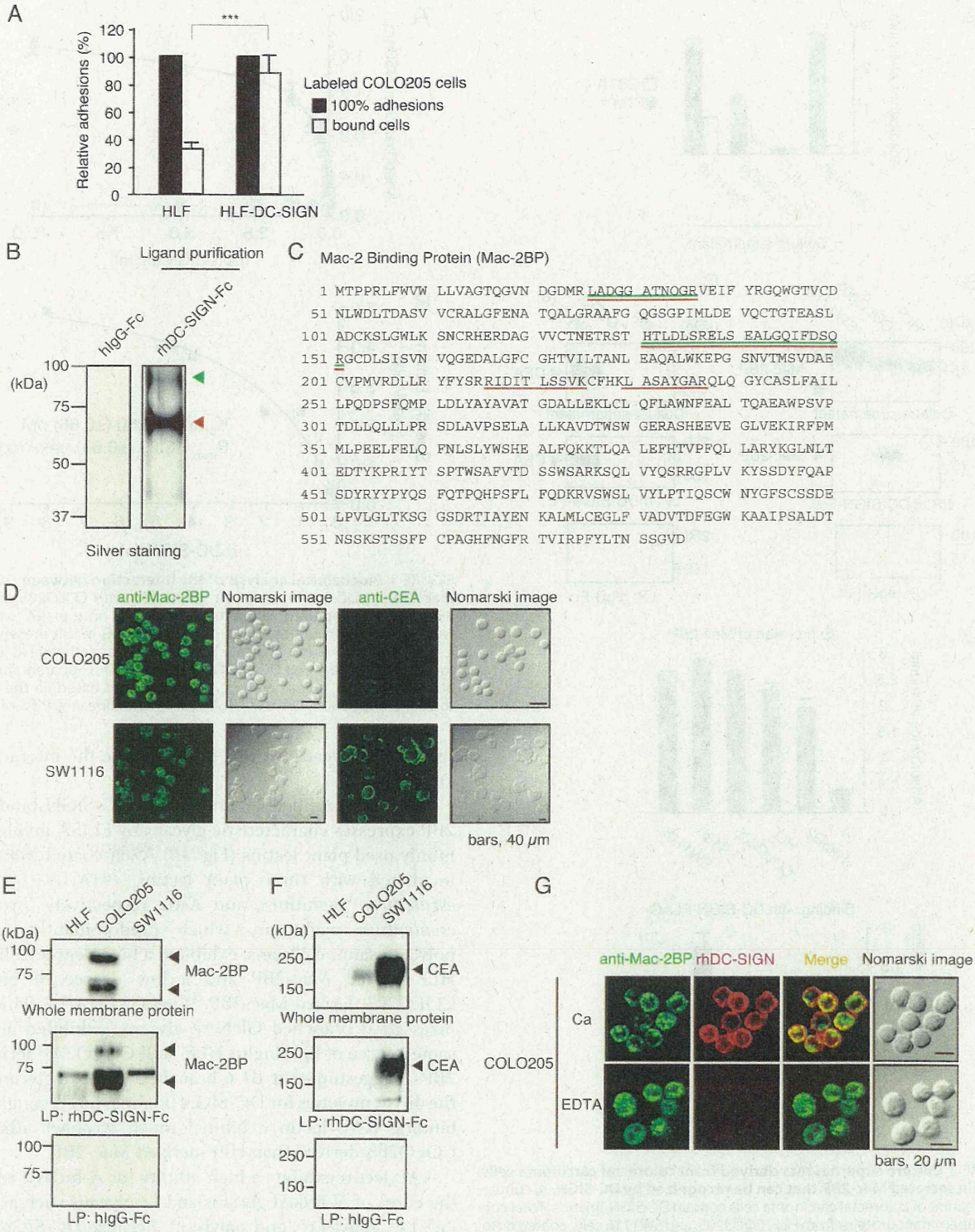

FIGURE 1. **Identification of Mac-2BP expressed on colorectal carcinomas as a novel ligand for DC-SIGN.** *A*, DC-SIGN-mediated cellular adhesions with COLO205 cells. HLF or HLF-DC-SIGN cells bound with calcein-AM-labeled COLO205 cells were lysed and analyzed by fluorometry at 488 nm. The relative adhesions are shown. *Error bars* indicate S.D. ($n = 3$). *B*, purification of DC-SIGN ligands expressed on COLO205 cells. DC-SIGN ligands were purified with a DC-SIGN affinity column and then detected by silver staining. The *arrowheads* indicate the elution positions of the purified DC-SIGN ligands. The molecular mass markers are shown on the *left*. *C*, identification of DC-SIGN novel ligands by MS. The purified DC-SIGN ligand bands were analyzed by MS. The identified peptides are shown in *green* (*upper band*) or *red* (*lower band*), respectively. *D*, confocal microscopic images of the expressions of Mac-2BP and CEA on COLO205 and SW1116 cells. Cells were stained with anti-Mac-2BP pAb or anti-CEA mAb (*green*). Nomarski images are shown on the *right*. *E* and *F*, ligand precipitation (*LP*) analysis of the interaction of DC-SIGN with CEA or Mac-2BP. Solubilized membrane proteins of HLF, COLO205, and SW1116 cells were precipitated with rhDC-SIGN-Fc or hIgG-Fc, and then EDTA-eluted DC-SIGN ligands were detected by immunoblotting using anti-Mac-2BP pAb (*E*) or anti-CEA mAb (*F*). *G*, confocal microscopic images of the interactions between DC-SIGN and Mac-2BP on COLO205 cells. The cells were costained with anti-Mac-2BP pAb (*green*) and rhDC-SIGN-allophycocyanin (*red*) in the presence of $CaCl_2$ or EDTA.

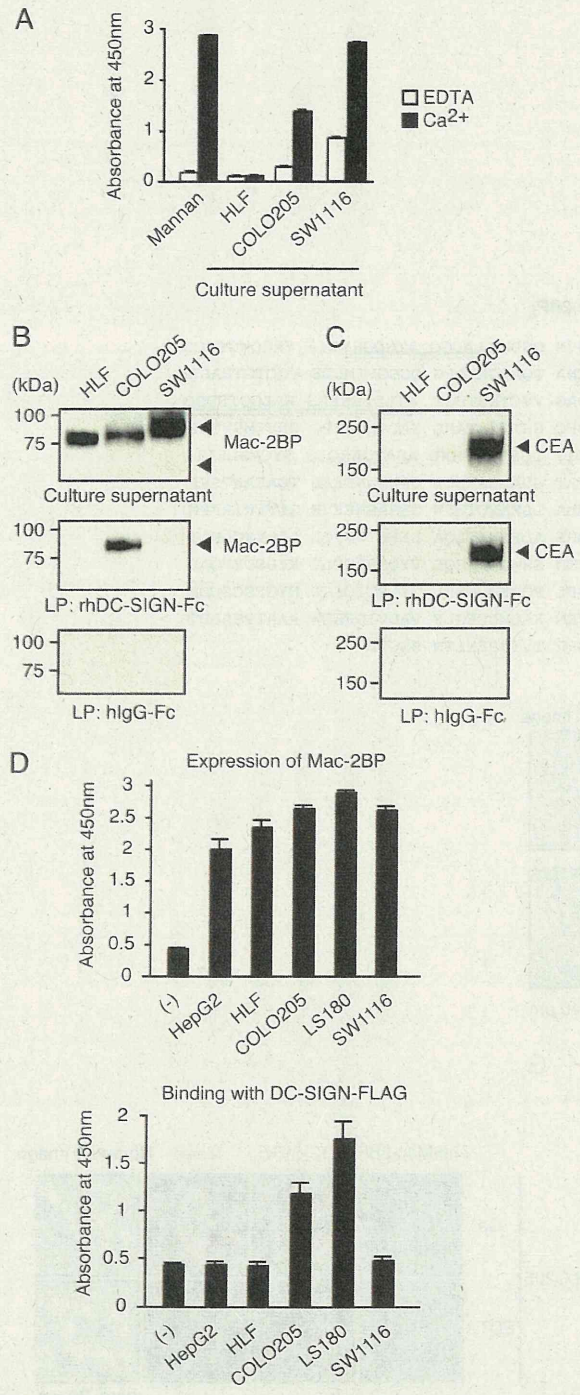

FIGURE 2. **Culture supernatants derived from colorectal carcinoma cells contain secreted Mac-2BP that can be recognized by DC-SIGN.** *A*, culture supernatant of colorectal carcinoma cells contain DC-SIGN-ligands. Total culture supernatant proteins from HLF, COLO205, and SW1116 cells, coated onto plates, were detected with rhDC-SIGN in the presence of 5 mM $CaCl_2$ or EDTA. Mannan was used as a positive control for DC-SIGN binding. *Error bars* indicate S.D. ($n = 3$). *B* and *C*, DC-SIGN interacts selectively with COLO205-derived Mac-2BP or SW1116-derived CEA contained in culture supernatants. A total culture supernatant and purified DC-SIGN ligands from HLF, COLO205, or SW1116 cells were immunoblotted with anti-Mac-2BP pAb or anti-CEA mAb. *D*, colorectal carcinoma cells secrete Mac-2BP that can be recognized by DC-SIGN. Mac-2BPs from human hepatoma HepG2 and HLF and colorectal carcinoma COLO205, LS180, and SW1116 cells were captured with anti-Mac-2BP pAb and then detected with anti-Mac-2BP mAb (*upper panel*) or with rhDC-SIGN-FLAG (*lower panel*), respectively. *Error bars* indicate S.D. ($n = 3$).

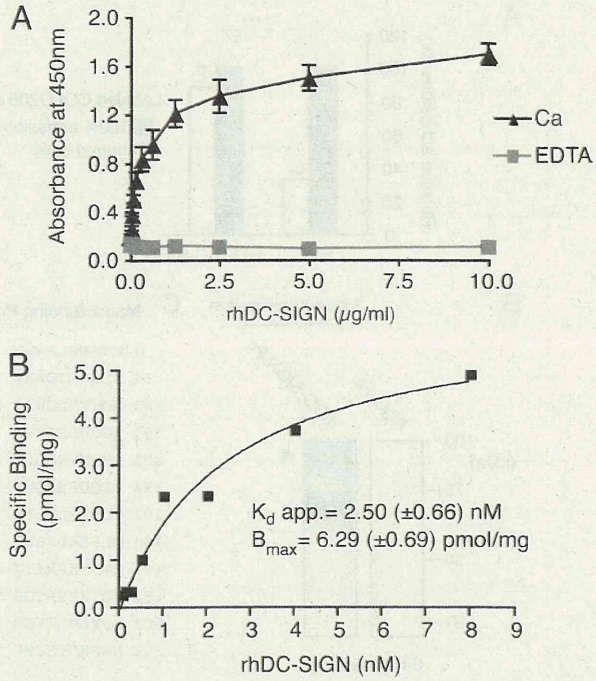

FIGURE 3. **Biochemical analysis of the interaction between DC-SIGN and Mac-2BP.** *A*, DC-SIGN-dependent interaction with COLO205-derived Mac-2BP. Mac-2BP, captured with anti-Mac-2BP pAb onto plates, was detected with different concentrations of rhDC-SIGN-FLAG in the presence of 5 mM $CaCl_2$ or EDTA. *Error bars* indicate S.D. ($n = 3$). *B*, quantitative kinetic analysis for association between DC-SIGN and Mac-2BP. The apparent (*app.*) dissociation constant (K_d app.) and B_{max} were calculated based on the amounts of total and unbound rhDC-SIGN-FLAG using a nonlinear regression model.

that the *N*-glycans on Mac-2BP mediate the interaction with DC-SIGN.

We next examined whether or not DC-SIGN-binding Mac-2BP expresses characteristic glycans by ELISA involving commonly used plant lectins (Fig. 4*B*). Well-coated Mac-2BP was incubated with three plant lectins, PHA-L4, *Lycopersicon esculentum* agglutinin, and AAL, respectively. *Lycopersicon esculentum* agglutinin, which predominantly recognizes polylactosamine glycans, exhibited a high degree of binding to HLF-derived Mac-2BP and a low degree of binding to COLO205-derived Mac-2BP. Whereas PHA-L4, which recognizes β1-6 branched GlcNAc glycans, exhibited almost the same degree of binding to HLF- and COLO205-derived Mac-2BPs, suggesting that β1-6 branched GlcNAc glycans are not the direct moieties for DC-SIGN binding. Interestingly, fucose-binding AAL lectin exhibited much stronger affinity with COLO205-derived than HLF-derived Mac-2BP.

AAL lectin exhibits a high affinity for α-fucosyl residues in the cores of *N*-linked glycans and Le glycans such as Le^a, Le^b, Le^x, Le^y, sialyl-Le^x, and sialyl-Le^x. Because DC-SIGN exhibits the highest affinity to Le glycans, but not to sialylated Le glycans, we hypothesized that fucose residues on Le glycans may directly mediate the interaction between DC-SIGN and COLO205-derived Mac-2BP. To prove this, we treated Mac-2BP with α1-3,4-fucosidase, an enzyme that specifically cleaves α1-3,4-bound fucose of Le^a, Le^b, Le^x, and Le^y. As shown in Fig. 4*C*, the defucosylated Mac-2BP had almost completely lost the ability to interact with DC-SIGN. Confocal microscopy also

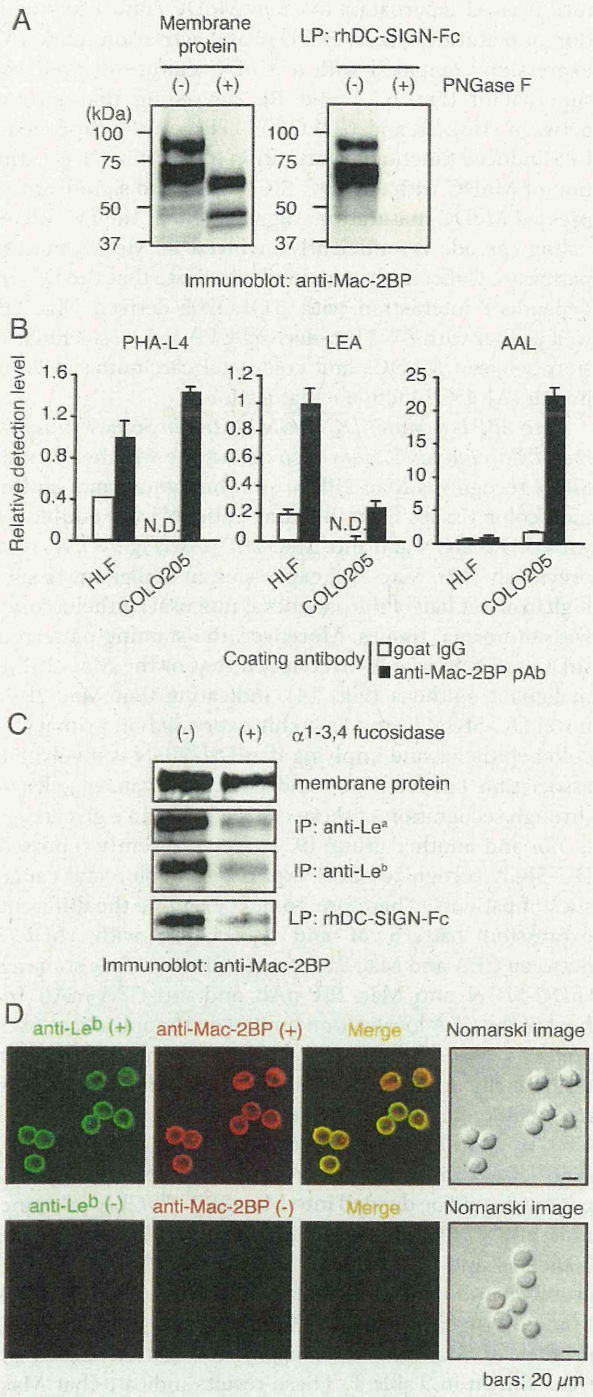

FIGURE 4. **Fucose residues of colorectal carcinoma-associated Lewis *N*-glycans expressed on COLO205-derived Mac-2BP are essential for DC-SIGN binding.** *A*, *N*-glycans of COLO205-derived Mac-2BP are essential for DC-SIGN binding. COLO205 membrane proteins were incubated with or without PNGase F, and then total membrane proteins (*left*) and subsequently purified DC-SIGN-ligands (*right*) were immunoblotted with anti-Mac-2BP pAb. *B*, determination for the Mac-2BP glycan profile by ELISA. COLO205-derived Mac-2BP glycoproteins captured with pre-coated anti-Mac-2BP pAb were detected with biotinylated plant lectin PHA-L4 (*left*), *Lycopersicon esculentum* agglutinin (*LEA*, *middle*), or AAL (*right*). Goat IgG was used as an isotype control for anti-Mac-2BP capture pAb. Detection levels for HLF-derived Mac-2BP were arbitrarily set at 1. *Error bars* indicate S.D. ($n = 3$). *C*, DC-SIGN recognizes the fucose residues of Le glycans expressed on COLO205-derived Mac-2BP. COLO205 membrane proteins were incubated with or without α1-3,4-fucosidase and then precipitated with rhDC-SIGN-Fc, anti-Le^a or -Le^b mAb, followed by immunoblotting with anti-Mac-2BP pAb. *IP*, immunoprecipitation. *D*, confocal microscopic image of Le^b expression on COLO205-derived Mac-2BP. The cells were costained with anti-Le^b mAb (*green*) and anti-Mac-2BP pAb (*red*). Staining without primary Abs was performed as a negative control. *LP*, ligand precipitation.

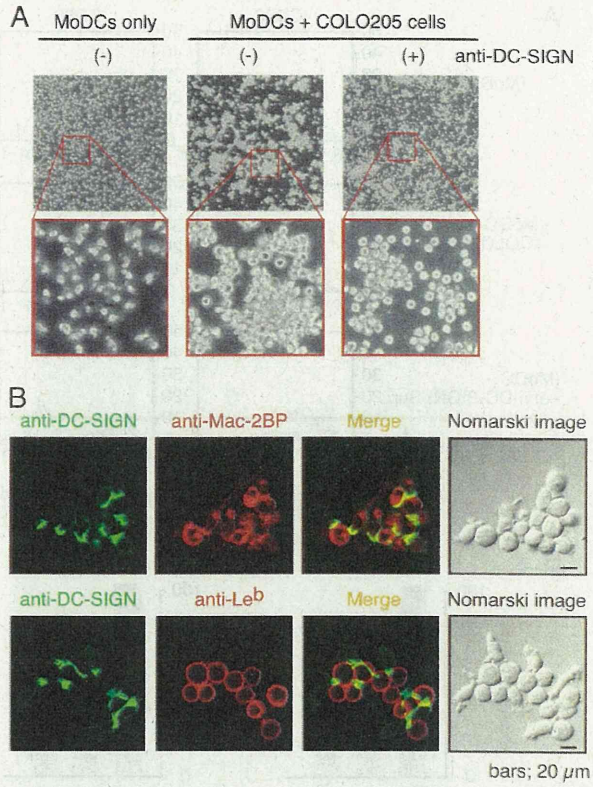

FIGURE 5. **DC-SIGN mediates interaction between MoDCs and COLO205 cells.** *A*, DC-SIGN-dependent cellular adhesions between MoDCs and COLO205 cells. MoDCs only (*left*) or MoDCs plus COLO205 cells in the presence (*right*) or absence (*middle*) of anti-human DC-SIGN pAb were cultured and visualized by phase-contrast microscopy. *B*, confocal microscopic images of MoDC-COLO205 cellular interactions mediated by DC-SIGN and Mac-2BP. MoDCs were cocultured with COLO205 cells. After fixation, cells were stained with anti-human DC-SIGN mAb (*green*) and anti-Mac-BP pAb or anti-Le^b mAb (*red*).

showed that Mac-2BP (*red*) significantly expresses Le^b glycans (*green*) on COLO205 cells (Fig. 4*D*). These results suggest that DC-SIGN is selective in its recognition of specific types of fucosylated *N*-glycans and that these *N*-glycans expressed on DC-SIGN-binding Mac-2BP are important for the interaction.

DC-SIGN Mediates Cellular Adhesion between Immature MoDCs and COLO205 Cells—Next, to determine whether or not immature DCs interact with COLO205 cells through DC-SIGN, we prepared MoDCs from human peripheral blood monocytes and cocultured them with COLO205 cells. As shown in Fig. 5*A*, MoDCs were found to stably adhere to COLO205 cells and to form large agglutinations when they were cocultured (*middle*), compared with a MoDC culture control (*left*). The addition of anti-DC-SIGN pAb partially blocked the MoDC-COLO205 interactions and agglutinations (*right*), indicating that DC-SIGN mediated the interactions and agglutinations. Furthermore, confocal microscopy demonstrated that immature MoDCs expressed a remarkable level of DC-SIGN (*green*) at the points of contact with COLO205 cells

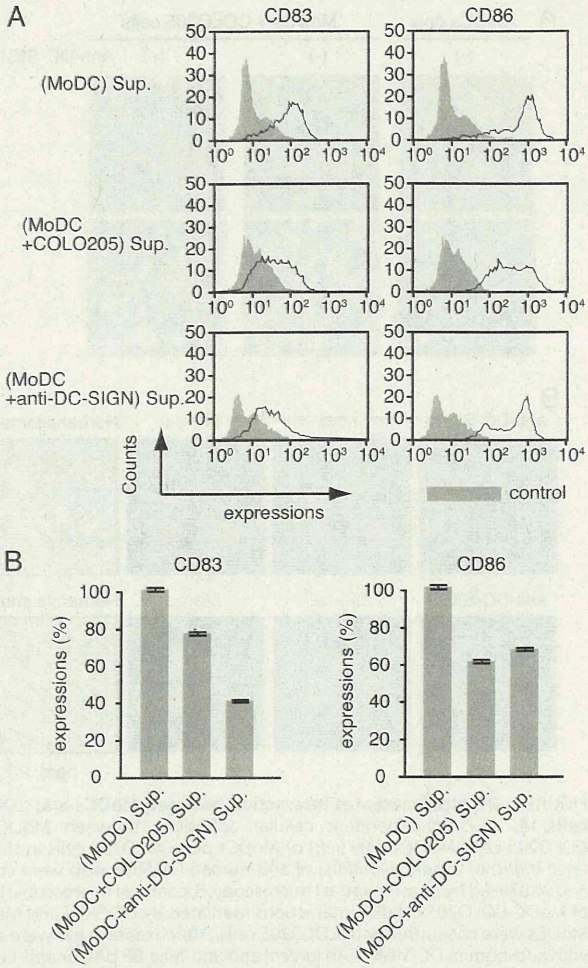

FIGURE 6. **A COLO205-MoDC coculture-derived supernatant suppresses the functional maturation of MoDCs.** *A*, flow cytometry analysis of CD83 and CD86 expressions. Immature MoDCs were incubated with a MoDC-cultured or COLO205-MoDC-cocultured supernatant (*Sup.*) for 3 days in the presence of IL-4, GM-CSF, and LPS (1 ng/ml), and the cultures were replenished with fresh supernatant on the second day. Supernatant of MoDCs, which cultured in the presence of anti-DC-SIGN pAb, was used as a control. The effect on MoDC functional maturation was determined as MoDC surface expression of CD83 and CD86 determined by flow cytometry. *B*, the relative expression levels of CD83 and CD86. The inhibition of MoDC functional maturation was measured as the percentage of mean fluorescent intensity (± S.E.) of incubation with MoDC-cultured supernatant. All experiments were performed in triplicate and were repeated a minimum of three times.

expressing both Mac-2BP (*upper*) and Le^b (*lower, red*) (Fig. 5*B*). These results, also considering the results of Fig. 4, *C* and *D*, suggest that Mac-2BP carrying Le^b glycans is involved in the association between MoDCs and colorectal cancer cells *in situ*.

DC-SIGN-mediated Cellular Adhesion between Immature MoDCs and COLO205 Cells Attenuates MoDC Maturation—We previously demonstrated that the MoDC-SW1116 adhesion mediated by the glycosylation-dependent interactions between DC-SIGN and CEA resulted in dysfunctional MoDCs (9, 10). To determine whether or not this observation is also caused by the DC-SIGN-Mac-2BP interaction, we examined the effect of MoDC-COLO205 coculture condition on MoDC functional maturation. A coculture-derived supernatant was prepared from cocultures of COLO205 carcinoma cells and MoDCs after LPS stimulation. The addition of the MoDC-COLO205 coculture-derived supernatant to a new MoDC culture led to inhibition of maturation marker CD83 and activation marker CD86 expression compared with a MoDC culture-derived control supernatant (Fig. 6, *A* and *B*), suggesting that interaction between MoDCs and COLO205 cells causes suppression of LPS-induced functional maturation of MoDCs. Direct stimulation of MoDC with anti-DC-SIGN pAb also significantly suppressed MoDC maturation, suggesting that the DC-SIGN signaling cascade is sufficiently involved in MoDC maturation pathways. Collectively, our results indicate that the DC-SIGN-dependent interaction with COLO205-derived Mac-2BP as well as that with SW1116-derived CEA induces cellular adhesion between MoDCs and colorectal carcinoma cells, which impairs MoDC functional maturation.

Mac-2BP Is a Major DC-SIGN Ligand in Some Primary Colorectal Carcinoma Tissues—To determine whether or not DC-SIGN recognizes Mac-2BP *in situ*, human normal and malignant colon tissues from the same patients were double stained with rhDC-SIGN and anti-Mac-2BP pAb (Fig. 7*A*). As reported previously (12), Mac-2BP expression in malignant tissues was high in about half of the patients at mucosal epithelia compared with in normal tissues. Moreover, the staining pattern in the rhDC-SIGN markedly overlapped that of the Mac-2BP in the malignant epithelia (Fig. 7*A*), indicating that Mac-2BP, as a novel DC-SIGN ligand, is highly expressed on primary cancer colon epithelia, and implying that DC-SIGN is involved in the association between DCs and colorectal cancer cells *in situ* through recognition of these cancer-related Le glycan ligands.

We and another group (9, 10) have recently reported that DC-SIGN recognizes CEA expressed in colorectal cancer tissues of patients. Therefore, to next examine the differences in expression pattern of and association with rhDC-SIGN between CEA and Mac-2BP, we performed triple staining with rhDC-SIGN, anti-Mac-2BP pAb, and anti-CEA mAb. In contrast to the CEA localization limited on the apical face of cancer epithelia, Mac-2BP expression exhibited a more diffuse pattern on both the apical and basolateral faces of epithelia in malignant colorectal cancer tissues, and little expression of either CEA or Mac-2BP was observed in colorectal normal tissues (Fig. 7*B*). Additionally, as shown in Fig. 7*B*, colorectal cancer patients could be divided into $Mac\text{-}2BP^{high}/CEA^{high}$ (cancer 1), $Mac\text{-}2BP^{low}/CEA^{high}$ (cancer 2 and 3), $Mac\text{-}2BP^{high}/CEA^{low}$ (cancer 4 and 5), and $Mac\text{-}2BP^{low}/CEA^{low}$ (data not shown) groups based on the distinct expression patterns of CEA and Mac-2BP together with the DC-SIGN recognition model. The profiles of Mac-2BP/CEA expression pattern-based groups were shown in Table 1. These results indicate that Mac-2BP may become a novel potential colorectal cancer biomarker for some patients with CEA-low or -negative colorectal cancer.

DISCUSSION

During the neoplastic process in colon tissues, genetic or epigenetic gene alteration often accompanies changes in cell-surface glycans. Glycosylation changes during malignant transformation lead to tumor-specific carbohydrate structures that interact with C-type lectins on dendritic cells. In general, these changes have been associated with a poor prognosis, as they are linked to the aggressiveness and metastatic capacity of tumors.

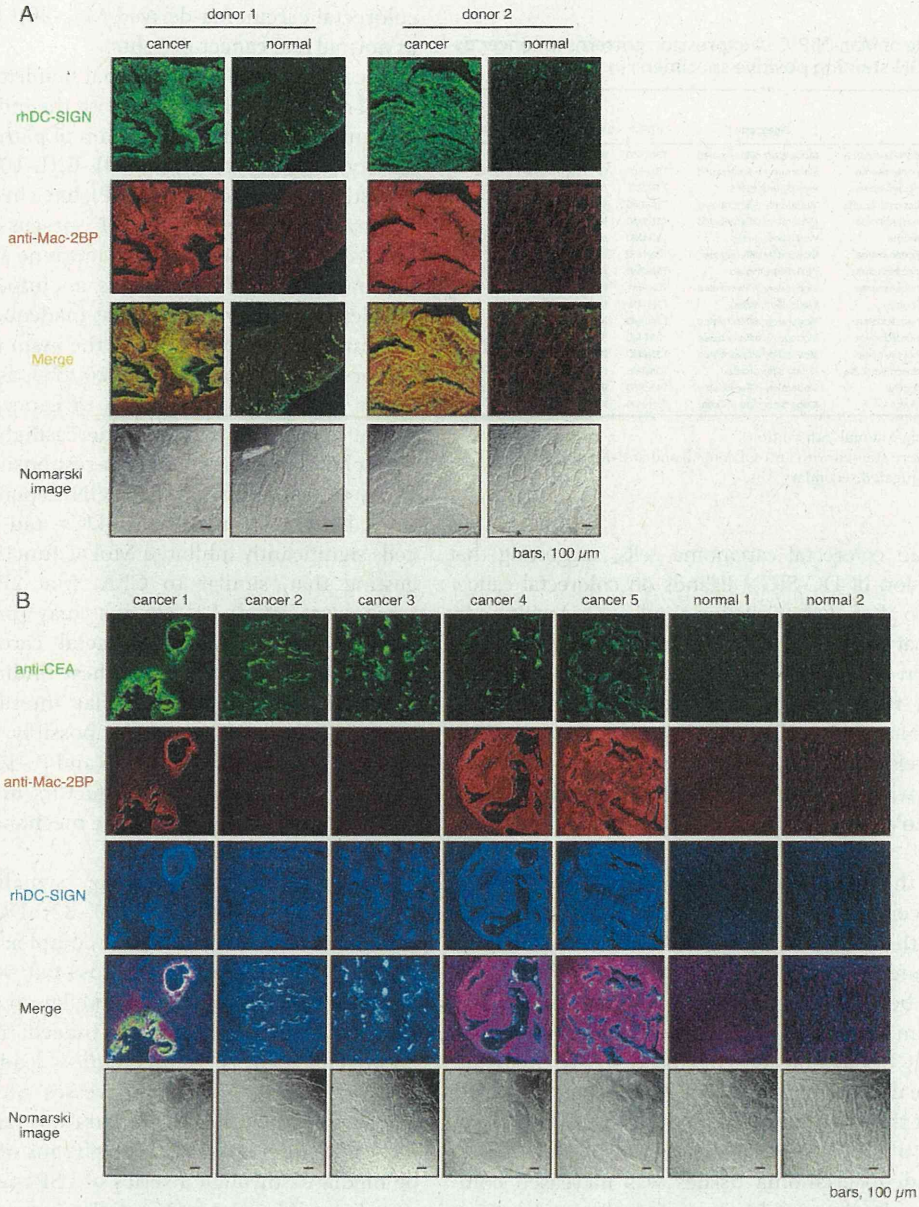

FIGURE 7. **Mac-2BP expressed on colorectal cancer cells is a major target for DC-SIGN *in situ*.** *A*, DC-SIGN recognizes colorectal carcinoma-derived Mac-2BP *in situ*. Primary colorectal cancer and normal colon tissues of donor 1 (SuperBioChips Laboratories) and donor 2 (Shiga University of Medical Science) were stained with rhDC-SIGN (*green*) and anti-Mac-2BP pAb (*red*). *B*, expressions of CEA and Mac-2BP in colorectal tumor tissues (SuperBioChips Laboratories). Triple staining of primary colorectal cancer and normal colon tissues with anti-CEA mAb (*green*), anti-Mac-2BP pAb (*red*), and rhDC-SIGN-allophycocyanin (*blue*). All samples were examined by confocal microscopy.

Good examples of heavily glycosylated tumor antigens are CEA and CEACAM1 (13–19), which can be secreted or expressed by colon cancer cells. Because the function of dendritic cells may be dependent on their binding properties as to self-antigens and pathogens, it is essential to obtain a detailed insight into the carbohydrate-binding properties of DC-SIGN.

Previous research indicated that tumor cells with their surface decorated with β1-6-branched *N*-linked oligosaccharides acquire invasiveness and metastatic potential through a change in the affinity level to the extracellular microenvironment (20, 21). Mac-2BP expressed on colorectal carcinoma cells was initially identified as a L-PHA-recognized major glycoprotein bearing polylactosamine glycans extending from β1-6 branched *N*-linked oligosaccharides (22, 23). In this study, we have firstly identified Mac-2BP on colorectal carcinoma cells as a novel ligand for C-type lectin DC-SIGN and demonstrated the Ca^{2+}-dependent interaction of rhDC-SIGN with Mac-2BP from colorectal carcinoma COLO205 cells. Generally, DC-SIGN exhibits dual specificities for high-mannose as well as Le-type glycans (8, 24, 25). Foreign antigens recognized by DC-SIGN have both types of glycans. Whereas, so far, most endogenous ligands for DC-SIGN have been found to carry only Le-type glycans. Here we showed that specific removal of Le glycans on Mac-2BP by α1-3,4-fucosidase abrogated these interactions, indicating that the fucose moieties of Le glycans are required for the interactions. We also observed that DC-SIGN ligands are highly expressed with Le